### MINIMIZING TRANSIENTS VIA THE KREISS SYSTEM NORM

#### PIERRE APKARIAN¹ AND DOMINIKUS NOLL²

ABSTRACT. We introduce system norms which assess transient behavior of stable Linear Time-Invariant (LTI) systems. This allows us to address undesired responses to initial conditions, finite resource consumption signals, or persistent perturbations. We then consider the challenging problem of minimizing these norms in closed loop using structured linear feedback. The computed controllers mitigate transients in a linearized closed loop, with the potential side effect of enlarging the region of stability of the underlying non-linear controlled system. In applications this helps to prevent transition to undesired nonlinear regimes, limit cycles or chaotic behavior. The success of our approach is certified a posteriori using Lyapunov-like techniques and simulations, as we demonstrate through a variety of applications.

KEY WORDS. Transient mitigation,  $L_1$  disturbances, Kreiss constant, structured controllers, non-smooth optimization, multi-objective optimization, suppression of attractors, LMI design techniques.

#### 1. Introduction

It has been observed in the literature that the size of the region of attraction of a locally stable nonlinear system

$$\dot{x} = Ax + \phi(x), \quad x_0 := x(0) := x(t=0),$$
 (1)

with  $\phi: \mathbb{R}^n \to \mathbb{R}^n$  is a static, memoryless nonlinearity with  $\phi(0) = 0$ ,  $\phi'(0) = 0$ , may strongly depend on the degree of normality of A. When A is far from normal, the linearization  $\dot{x} = Ax$ ,  $x(0) = x_0$ , may have large transient peaks, which may incite trajectories of (1) to leave the region of attraction. This is known as *peaking*, [1, 2, 3, 4, 5], and considered a major obstacle to global stability.

The tendency of a stable A to produce large transients or peaking may be assessed by its worst-case transient growth

$$M_0(A) = \max_{t \ge 0} \max_{\|x_0\|_2 = 1} \|e^{At} x_0\|_2 = \max_{t \ge 0} \overline{\sigma}(e^{At}), \tag{2}$$

and in closed loop, when A depends on tunable parameters, one may minimize  $M_0(A_{cl})$  in order to enlarge the region of local stability of (1). This has been studied in [6] for structured controllers, and previously in [7] using the controller Q-parametrization.

In a continuous operating process the effect of initial values is not the appropriate lever, as instability is caused rather by noise, persistent perturbations, or finite-consumption disturbances. Moreover, nonlinearity often arises only in some of the states z, and likewise may affect only parts of the dynamics, and we address those issues by considering as a

<sup>&</sup>lt;sup>1</sup>ONERA, Department of System Dynamics, Toulouse, France.

<sup>&</sup>lt;sup>2</sup>Institut de Mathématiques, Université de Toulouse, France.

refined version of (1) a nonlinear controlled system of the form

$$\dot{x} = Ax + B\phi(z) + Bw + B_u u$$

$$z = Cx$$

$$y = C_u x$$
(3)

with  $x \in \mathbb{R}^n$ ,  $u \in \mathbb{R}^m$ ,  $y \in \mathbb{R}^p$ ,  $w \in \mathbb{R}^{m_w}$ ,  $z \in \mathbb{R}^{p_z}$ , where the non-linearity  $\phi : \mathbb{R}^{p_z} \to \mathbb{R}^{m_w}$  satisfies  $B\phi(0) = 0$  and  $B\phi'(0)C = 0$ , and where a tunable feedback controller  $u = K(\mathbf{x})y$ , with  $\mathbf{x}$  as decision variables, is sought which stabilizes the system locally, rendering it as resilient as possible with regard to these disturbances. The latter is aimed at indirectly by tuning the closed loop channel  $w \to z$  to remain small with regard to a system norm assessing transients, the idea being that disturbances w cause the partial state z to have unduly large transients.

Closing the loop with respect to the controller  $K(\mathbf{x})$  in (3), we consider the linear closed-loop channel  $T_{wz}(\mathbf{x}, s) = C(sI - A_{cl}(\mathbf{x}))^{-1}B$ , which we now tune in such a way that transients in z(t) due to disturbances w(t) remain small. Expanding on (2), we assess transients of  $G(s) = C(sI - A)^{-1}B$  via

$$\mathcal{M}_0(G) = \sup_{t \ge 0} \overline{\sigma} \left( C e^{At} B \right) = \sup_{\|w\|_1 \le 1} \|G * w\|_{\infty}, \tag{4}$$

a time-domain  $L^1 \to L^{\infty}$  induced system norm, which measures the time-domain peak of the response z = G \* w to a finite consumption input w. For  $G(s) = (sI - A)^{-1}$  we recover  $\mathcal{M}_0(G) = M_0(A)$ .

The principal goal of this contribution is to develop a closed-loop controller design technique, which mitigates transients of (3) via the indicated heuristic, performs fast and reliably, and at the same time can be combined with standard design specifications in robust control. In addition, this should be achieved with simple and practically useful controller structures commonly used in engineering designs.

In order to achieve this goal, we rely on frequency domain techniques, which leads us to introduce the Kreiss system norm  $\mathcal{K}(G)$  as a frequency domain approximation to (4), the definition being given in Section 2. The fact that  $\mathcal{K}(G)$  is frequency-based offers algorithmic advantages for optimization and combines favorably with classical frequency-domain specifications, such as stability margins, noise and disturbance attenuation, loop shaping constraints, allowing realistic and practically relevant design settings. A challenge is that this leads to multi-objective optimization programs with non-smooth criteria and constraints.

Along with disturbances of finite consumption,  $w \in L^1$ , it also makes sense to consider finite energy perturbations  $w \in L^2$ , which may be thought of as representing noise, or time-domain bounded  $w \in L^{\infty}$ , which stand for persistent perturbations, as naturally all those could be the reason why trajectories of (1) or (3) get outside the region of attraction. Ability of a system to withstand destabilizing disturbances is referred to as resilience, and along with  $\mathcal{M}_0(G)$  or  $\mathcal{K}(G)$  other ways to quantify it have been discussed, see e.g. [8]. Resilience of systems is currently a subject of broad interest and addressed in various ways, see e.g. [9, 10, 11, 12].

In parallel with (4), where peaking is quantified in the time-domain  $L^{\infty}$ -norm in response to finite consumption inputs, dissipative system theory assesses transient responses to initial values in the energy norm [13, 14, 15, 16]. While related, there is no direct link between these concepts. Yet it is worth mentioning that dissipativity analysis based on quadratic storage functions may be cast as integral quadratic constraints (IQCs), see [17]. In analysis, those lead to linear matrix inequalities (LMIs), but in synthesis turn into bilinear matrix inequalities (BMIs), which are non-convex and often cumbersome to solve

due to the large number of optimization variables. This is why alternative more successful ways to address IQCs have been proposed, see [18, 19, 20].

There are cases where applying dissipativity theory to a nonlinear system with a static nonlinearity can be turned into LMI synthesis conditions. This occurs in the application of section 7, where the structure of the nonlinearity admits a simple characterization via quadratic constraints. In this setting, no multipliers are required and the synthesis conditions can be reduced to LMIs in the same vein as in [21, 22]. These conditions may be conservative and should therefore be evaluated in the context of each specific application. It should be emphasized that this approach does not provide a means to prescribe or restrict the structure of the controller.

Mitigating large transients is a general concern in control design, and has been addressed e.g. in [23, 24, 25, 26]. LMI approaches are discussed in [27, 28], and a comparison between minimization of (4) and LMI techniques is [29], suggesting that, in the case of plane Poiseuille flow, minimization (4) may be less conservative.

The remainder of this article is organized as follows. Section 2 introduces the Kreiss system norm  $\mathcal{K}(G)$  as a frequency domain approximation of  $\mathcal{M}_0(G)$ , followed by Section 3, which presents the central Kreiss optimization program. Section 4 gives norm estimates related to  $L_1$ -disturbances. Section 4.1 derives the system norm estimate  $\mathcal{K}(G) \leq \mathcal{M}_0(G)$  from Young's inequality. In Section 4.2 we investigate attainment of the lower bound  $\overline{\sigma}(CB) \leq \mathcal{K}(G) \leq \mathcal{M}_0(G)$ . This is important in view of the quest whether lack of normality of the system A-matrix continues to be the cause of unduly large transients when the set-up is (3) and no longer (1). Section 5.3 addresses the case of persistent perturbations, again using Young's inequality. Experiments in Sections 6 and 7 focus on  $L_1$ -disturbances, where we apply the Kreiss norm minimization of Section 2 to control nonlinear dynamics involving limit cycles, chaos or multiple fixed points, with the goal to mitigate transients and thereby increase the region of local stability or to even achieve global stability in closed loop. Conclusions are given in Section 8.

### NOTATION

Notation is standard. Time-domain  $L^p$ -spaces are equipped with classical signal norms as in [30]. Time and Laplace variables are t and s, and Re(.) denotes the real part, \* is convolution. For matrices M symbols  $M^T$ ,  $M^H$ ,  $M^{-1}$ ,  $\mathrm{Tr}(M)$  mean transpose, conjugate transpose, inverse and trace,  $I_n$  stands for the identity matrix of size n. We use  $\mathrm{diag}(A_1,A_2)$  to denote a block-diagonal matrix with blocks  $A_1$  and  $A_2$ . For Hermitian matrices,  $M \succ N$  means M-N is positive definite,  $M \succeq N$  means M-N is positive semi-definite. Maximum singular values and maximum eigenvalues are denoted  $\overline{\sigma}$  and  $\overline{\lambda}$ . The matrix exponential is  $e^A$ . The  $H_{\infty}$ -norm of a transfer function G(s) is denoted  $\|G\|_{\infty}$  or  $\|G(s)\|_{\infty}$ . The Clarke directional derivative of a locally Lipschitz function f is f'(x,d), the Clarke sub-differential is  $\partial f(x)$ ; [31]. The adjoint of a linear operator T is  $T^*$ . Additional specific notations are introduced within the text.

## 2. Kreiss system norm

As observed in [32], it may be difficult to compute  $M_0(A)$  and  $\mathcal{M}_0(G)$  fast and accurately enough for the purpose of optimization. In response, the authors of [32] propose to use the *Kreiss constant* K(A) of a matrix  $A \in \mathbb{R}^{n \times n}$  as an alternative measure of normality. The latter is defined as

$$K(A) = \max_{\operatorname{Re}(s)>0} \operatorname{Re}(s)\overline{\sigma}\left((sI - A)^{-1}\right),\tag{5}$$

and its computation was investigated in [33, 34, 6]. By the famous Kreiss Matrix Theorem [35, p. 151, p.183] the estimate

$$K(A) < M_0(A) < enK(A) \tag{6}$$

is satisfied with e = 2.7183.. the Euler number and n the matrix size, where the right hand estimate is generally pessimistic, but sharp as shown in [32].

In view of (6) minimizing  $K(A_{\rm cl})$  has an effect similar to minimizing  $M_0(A_{\rm cl})$ , and this is in line with the observation that the global minimum  $K(A) = M_0(A) = 1$  is the same for both criteria and occurs for normal A, and more generally, for matrices A where  $e^{At}$  is a contraction in the spectral norm. In [6] we have shown that optimizing  $K(A_{\rm cl})$  is numerically possible, and that it has indeed the desired effect of driving  $A_{\rm cl}$  closer to normal behavior. This has incited a vivid interest in Kreiss constant minimization, see e.g. [36, 37, 38, 39, 40, 41].

Expanding to (3) requires computation and optimization of  $\mathcal{M}_0(G)$ , which in closed loop encounters similar difficulties. We therefore introduce the Kreiss system norm

$$\mathcal{K}(G) := \sup_{\text{Re}(s) > 0} \text{Re}(s) \overline{\sigma} \left( C(sI - A)^{-1} B \right),$$

which generalizes K(A) in a natural way and satisfies the same estimate

$$\mathcal{K}(G) \le \mathcal{M}_0(G) \le en \,\mathcal{K}(G),$$
 (7)

as we shall prove in Section 4.1. The principled reason to use  $\mathcal{K}(G)$  is that its computation, and for that matter, optimization, may be based on a robust control technique, first proposed in [6, Thm. 2.1] for the case  $B = C = I_n$ :

**Lemma 1.** Suppose A is stable. Then the Kreiss system norm K(G) can be computed through the robust  $H_{\infty}$ -performance analysis program

$$\mathcal{K}(G) = \max_{\delta \in [-1,1]} \left\| C \left( sI - \left( \frac{1-\delta}{1+\delta} A - I \right) \right)^{-1} B \right\|_{\infty}, \tag{8}$$

where  $||G||_{\infty}$  denotes the  $H_{\infty}$ -system norm.

The Kreiss norm can be computed either by solving a nonsmooth max-max program, or by a convex Semi-Definite Program (SDP); see [6, Theorems 2.1 and 2.4] and the discussion given there. The SDP provides a certified accuracy and accounts for the worst case complexity, but the nonsmooth technique is considerably faster. In numerical testing, we therefore use the SDP only for the final certification.

# 3. Kreiss norm minimization

This leads us now to the following synthesis program:

minimize 
$$\mathcal{K}(T_{wz}(\mathbf{x}))$$
  
subject to  $K(\mathbf{x})$  stabilizing  $\mathbf{x} \in \mathbb{R}^n$  (9)

where  $\mathbf{x} \in \mathbb{R}^n$  are the finitely many tunable parameters of the structured controller  $K(\mathbf{x})$ , and where  $T_{wz}(\mathbf{x}, s)$  is the linear closed-loop channel of (3), by which we assess transients. In practice program (9) will be complemented by adding standard  $H_{\infty}$ - or  $H_2$ -loop-shaping requirements as constraints to further improve performances and robustness, as for instance explained in [42, 43, 44]. Examples are (17) and (34) in Sections 6 and 7.

Program (9) is a special case of a much wider class of problems with parametric uncertainty discussed in [43, 44]. Computation of  $\mathcal{K}(T_{wz}(\mathbf{x}))$  in closed loop involves system matrices of size  $N := n + n_K$ , with n the order of the plant,  $n_K$  the controller state

dimension, and is of the order  $O(N^3)$  mainly through Hamiltonian eigenvalue computations. The same complexity applies to computing transfer functions. Clarke subgradients of criteria and constraints use [43, Sect. IV, Prop. 1] and are of the order  $O(p_z^3 + m_w^3 + n_K^3)$ , which gives some speedup of (3) over (1). Some experiments are documented in [29, 6].

Further information in the assessment of (9) concerns the number of iterations required by the optimizer. Since design problems are non-convex, we content ourselves with local minima, which is beneficial as finding global minima is NP-hard and computationally infeasible for sizable problems. Non-smoothness of criteria and constraints complicates matters, and in response is addressed by tailored optimization techniques, [45, 46]. An advantage of our approach is that it avoids the use of Lyapunov variables, so that the number of decision variables is typically way smaller than the matrix dimension,  $\dim(\mathbf{x}) \ll$  $n + n_K$ . This is significant, because each optimization step calls for a convex quadratic program with size  $\dim(\mathbf{x})$  and computational complexity  $O(\dim(\mathbf{x})^3)$ . Altogether the optimizer succeeds for medium size problems consistently under 100 iterations.

Comparisons in [6] show that LMI-based methods fail much earlier when the matrix dimension increases. Recent experiments in the literature as well as our own in Sections 6 and 7 indicate that  $N = n + n_K$  is the dominant parameter.

### Organization of the theoretical contribution

In the following two sections we discuss theoretical aspects of disturbances causing large transients via peaking. This includes:

**Section 4:** Finite consumption disturbances and norm estimates relating time and frequency domain via Young's inequality:

- Estimate for the Kreiss system norm (Section 4.1),
- Question of attainment of the lower bound of  $\mathcal{K}(G)$  and the role of normality of the system A-matrix (Section 4.2).
- Hausdorff's numerical abscissa extended to systems (Section 4.3).

**Section 5:** System norms other than  $\mathcal{M}_0(G)$ ,  $\mathcal{K}(G)$  which assess peaking:

- Alternative computable frequency based system norms (Sections 5.1, 5.2).
- Peak gain norm for persistent perturbations and estimate relating it to the  $H_{\infty}$ -norm via Young's inequality.
- $L^2 \to L^2$  operator norm to address noise (Sections 5.4).

#### 4. Norm estimates

In this Section, we obtain basic estimates relating the Kreiss system norm  $\mathcal{K}(G)$  to the  $L^1 \to L^\infty$  induced norm  $\mathcal{M}_0(G)$ . We recall Young's inequality:

**Lemma 2.** (Young's inequality; see [47]). Let 1/p + 1/q + 1/r = 2,  $p, q, r \ge 1$ , and 1/p + 1/p' = 1. Then

$$\left| \iint f(x)g(x-y)h(y)dydx \right| \le C_p C_q C_r ||f||_p ||g||_q ||h||_r,$$

where

$$C_p = \left(p^{1/p}/p'^{1/p'}\right)^{1/2}, C_1 = C_{\infty} = 1.$$

Let  $\xi, \eta$  be test vectors of appropriate dimensions and consider a one-dimensional signal u(t), then Lemma 2 gives

$$\xi^{T}C(sI - A)^{-1}B\eta u(s) = \int_{0}^{\infty} e^{-st}(\xi^{T}Ce^{At}B\eta * u)(t)dt$$

$$\leq C_{p}C_{q}C_{r}\|e^{-st}\|_{p}\|\xi^{T}Ce^{At}B\eta\|_{q}\|u\|_{r}$$

$$= C_{p}C_{q}C_{r}\operatorname{Re}(s)^{-1/p}p^{-1/p}\|\xi^{T}Ce^{At}B\eta\|_{q}\|u\|_{r},$$
(10)

where  $f(t) = e^{-st}$ ,  $g(t) = \xi^T C e^{At} B \eta$ , and h(t) = u(t) are understood to take values 0 for t < 0. In the sequel we consider various choices of p, q, r.

4.1. Kreiss system norm. We apply Young's inequality with  $r=1, q=\infty, p=1$ , where  $C_pC_qC_r=1$ . This leads to the following

**Theorem 1.** For a stable system  $G(s) = C(sI - A)^{-1}B$  we have the estimate

$$\mathcal{K}(G) := \sup_{\operatorname{Re}(s) > 0} \operatorname{Re}(s) \overline{\sigma} \left( C(sI - A)^{-1} B \right) \le \sup_{t \ge 0} \overline{\sigma} \left( Ce^{At} B \right) =: \mathcal{M}_0(G). \tag{11}$$

**Proof:** From (10) with r = 1,  $q = \infty$ , p = 1, we get

$$\operatorname{Re}(s)|\xi^T C(sI - A)^{-1} B \eta u(s)| \le \|\xi^T C e^{At} B \eta\|_{\infty} \|u\|_{1}.$$

Now take  $u_{\epsilon}(t) = \epsilon^{-1}$  on  $[0, \epsilon]$ ,  $u_{\epsilon}(t) = 0$  else. Then  $||u_{\epsilon}||_1 = 1$ . On the other hand,  $u_{\epsilon}(s) \to 1$  as  $\epsilon \to 0$ , hence we get

$$\operatorname{Re}(s)|\xi^T C(sI - A)^{-1}B\eta| \le \|\xi^T Ce^{At}B\eta\|_{\infty} = \sup_{t>0} |\xi^T Ce^{At}B\eta|.$$

Now we consider test vectors  $\xi \in \ell_2$ ,  $\eta \in \ell_2$ . Passing to the supremum over  $\|\xi\|_2 \leq 1$ ,  $\|\eta\|_2 \leq 1$  on the right gives

$$\operatorname{Re}(s)|\xi^{T}C(sI - A)^{-1}B\eta| \leq \sup_{t\geq 0} \sup_{\|\xi\|_{2}, \|\eta\|_{2}\leq 1} |\xi^{T}Ce^{At}B\eta|$$
$$= \sup_{t\geq 0} \overline{\sigma} \left(Ce^{At}B\right).$$

Then taking the supremum over  $\|\xi\|_2 \le 1$ ,  $\|\eta\|_2 \le 1$  and Re(s) > 0 on the left gives

$$\mathcal{K}(G) = \sup_{\operatorname{Re}(s)>0} \operatorname{Re}(s)\overline{\sigma}\left(C(sI-A)^{-1}B\right) \le \sup_{t\ge 0} \overline{\sigma}\left(Ce^{At}B\right) = \mathcal{M}_0(G),$$

which is the claimed estimate.

In order to interpret the expression  $\mathcal{M}_0(G)$  on the right, we consider vector norms on  $L^p([0,\infty),\mathbb{R}^n)$  defined as

$$||u||_{p,q} = \left(\int_0^\infty |u(t)|_q^p dt\right)^{1/p},$$

where  $|u|_q = (\sum_{i=1}^n |u_i|^q)^{1/q}$  is the standard vector q-norm in  $\mathbb{R}^n$ , and where  $||u||_{\infty,q} = \sup_{t>0} |u(t)|_q$ . Then, with the terminology introduced in [30],

$$||G||_{(q,s),(p,r)} = \sup_{u \neq 0} \frac{||G * u||_{q,s}}{||u||_{p,r}}$$
(12)

are induced norms  $G:(L^p,\|\cdot\|_{p,r})\to (L^q,\|\cdot\|_{q,s})$ . In some cases these admit closed-form expressions, which is a prerequisite to making them amenable to computations, and even more so, optimization. By [30, (25)] one such case is

$$||G||_{(\infty,p),(1,r)} = \sup_{t \ge 0} ||G(t)||_{p,r}, \tag{13}$$

where  $||A||_{q,p} = \sup_{x\neq 0} ||Ax||_q/||x||_p$  are the usual well-known induced matrix norms. Therefore, if we choose p = r = 2 in (13), then

$$||G||_{(\infty,2),(1,2)} = \sup_{t\geq 0} ||G(t)||_{2,2} = \sup_{t\geq 0} \overline{\sigma}(G(t)) = \mathcal{M}_0(G).$$

We have proved

**Proposition 1.**  $\mathcal{M}_0(G)$  is an induced system norm. Given the vector input w(t) satisfying  $\int_0^\infty |w(t)|_2 dt = \int_0^\infty \left(\sum_{k=1}^p |w_k(t)|^2\right)^{1/2} dt = 1$ , it measures the output z = G\*w by the vector signal norm

$$\sup_{t \ge 0} \|z(t)\|_2 = \sup_{t \ge 0} \left( \sum_{i=1}^m |z_i(t)|^2 \right)^{1/2}.$$

The norm  $\mathcal{M}_0(G) = ||G||_{(\infty,2),(1,2)}$  will be called the worst case transient peak norm, as it measures the peak of the time-domain response of G to a signal with finite resource consumption. Here 'response to a signal of finite resource consumption' is terminology adopted from [48].

In consequence, the expression  $\mathcal{K}(G)$  is a frequency domain lower bound of  $\mathcal{M}_0(G)$ , and it is easy to see that  $\mathcal{K}(G)$  is a norm, which we will call the *Kreiss system norm*.

Remark 1. We do not expect  $\mathcal{K}(G)$  to be an induced system norm, but it does have the property of an operator norm, as follows from Theorem 1. Indeed, let  $G_{\delta} = C(sI - (\frac{1-\delta}{1+\delta}A - I))^{-1}B$ , then  $\|G_{\delta}\|_{\infty}$  is the  $L^2 \to L^2$  induced system norm when we take  $\|\cdot\|_{2,2}$  as vector norm. Hence  $\|z\|_{2,2} \leq \max_{\delta \in [0,1]} \|G_{\delta}\|_{\infty} \|w\|_{2,2}$ , which due to (8) gives  $\|G * w\|_{2,2} \leq \mathcal{K}(G) \|w\|_{2,2}$ .

**Remark 2.** Suppose G = (A, B, C) is output controllable. Then for  $y_0 \in \operatorname{im}(C)$ ,  $y_0 \neq 0$ , there exists  $u_0$  and  $t_0 > 0$  such that  $Ce^{At_0}Bu_0 = y_0$ . Then  $\mathcal{M}_0(G) \geq \overline{\sigma}(Ce^{At_0}B) \geq \|Ce^{At_0}Bu_0\|_2/\|u_0\|_2 = \|y_0\|_2/\|u_0\|_2 > 0$ . Some such condition is of course required, because if we take  $C = [1\ 1]$ ,  $B = \begin{bmatrix} 1 \\ -1 \end{bmatrix}$ ,  $A = -I_2$ , then  $Ce^{At}B = 0$  for all t.

**Remark 3.** The famous estimate (upper bound due to Spijker [49])

$$K(A) \le M_0(A) \le neK(A) \tag{14}$$

holds for matrices A of size  $n \times n$ , and the global minimum  $K(A) = M_0(A) = 1$  is attained for matrices where  $e^{At}$  is a contraction in the spectral norm, and in particular, for normal matrices. For this reason  $M_0(A)$ , and K(A), have been considered as 'measures of non-normality' of a matrix.

The following extends (14), obtained in [50, 32, 49], to system norms:

Theorem 2. We have

$$\mathcal{K}(G) \leq \mathcal{M}_0(G) \leq en \, \mathcal{K}(G).$$

**Proof:** We have already shown in Theorem 1 that  $\mathcal{K}(G) \leq \mathcal{M}_0(G)$ . For the upper bound estimate, take test vectors  $\xi, \eta$ , then on putting  $q(s) = \xi^T C(sI - A)^{-1} B \eta$ , we have

$$\xi^{T} C e^{At} B \eta = \frac{1}{2\pi j} \int_{\text{Re}(s)=\mu} e^{st} \xi^{T} C(sI - A)^{-1} B \eta \, ds \text{ (inverse Laplace)}$$

$$= -\frac{1}{2\pi j} \int_{\text{Re}(s)=\mu} \frac{e^{st}}{t} q'(s) ds \text{ (partial integration)}$$

$$= -\frac{1}{2\pi j} \frac{e^{\mu t}}{t} \int_{-\infty}^{\infty} e^{j\omega t} q'(\mu + j\omega) j \, d\omega$$

П

Using  $Re(s) = \mu = 1/t$  and taking absolute values, we obtain

$$|\xi^T C e^{At} B \eta| \le \frac{e}{2\pi} \frac{1}{t} \int_{-\infty}^{\infty} |q'(1/t + j\omega)| d\omega = \frac{e}{2\pi} \operatorname{Re}(s) \|q'(\operatorname{Re}(s) + j\cdot)\|_{1}.$$

Since by [49] and [32] we have  $||q'||_1 \le 2\pi n ||q||_{\infty}$ , we find

$$|\xi^T C e^{At} B \eta| \le en \operatorname{Re}(s) \sup_{\omega} |\xi^T C ((\operatorname{Re}(s) + j\omega)I - A)^{-1} B \eta|$$
  
$$\le en \sup_{\operatorname{Re}(s)>0} \operatorname{Re}(s) |\xi^T C (sI - A)^{-1} B \eta|,$$

so that taking the supremum over  $\|\xi\|_2 = 1$ ,  $\|\eta\|_2 = 1$  gives the right hand estimate.  $\square$ 

4.2. Attainment of the Kreiss lower bound. The fact that K(A) and  $M_0(A)$  attain their common global lower bound  $K = M_0 = 1$  for contraction semi-groups  $e^{At}$  in the spectral norm rises the question whether the situation for K(G) and  $\mathcal{M}_0(G)$  is similar. This is investigated in the present section. In particular, we ask whether a gap between K(G),  $\mathcal{M}_0(G)$  and their lower bound can still be attributed to non-normal behavior of the system A-matrix.

**Proposition 2.** We have the lower bound  $\overline{\sigma}(CB) \leq \mathcal{K}(G) \leq \mathcal{M}_0(G)$ .

**Proof:** For x > 0 we have  $\mathcal{K}(G) \ge x\overline{\sigma}(C(xI - A)^{-1}B) = \overline{\sigma}(Cx(xI - A)^{-1}B)$ , and since the matrix  $x(xI - A)^{-1}$  approaches I as  $x \to \infty$ , we get the lower bound  $\overline{\sigma}(CB)$  all right.  $\square$ 

For  $G = (sI - A)^{-1}$  this reproduces the bound  $K(A) \geq 1$ , which as we know is attained when  $e^{At}$  is a contraction in the spectral norm, and in particular, for normal matrices. The question is therefore whether, or for which systems G = (A, B, C), the bound  $\overline{\sigma}(CB)$  is attained. It is clear from Proposition 2 that  $\mathcal{M}_0(G) = \overline{\sigma}(CB)$  implies equality  $\overline{\sigma}(CB) = \mathcal{K}(G) = \mathcal{M}_0(G)$ . However, in the matrix case the reverse argument is also true, i.e., K(A) = 1 implies  $M_0(A) = 1$  as a consequence of the Hille-Yosida theorem [51]. The analogous result for systems is no longer valid.

**Example 1.** If we consider a stable SISO system

$$G(s) = \frac{c_{n-1}s^{n-1} + \dots + c_0}{s^n + a_{n-1}s^{n-1} + \dots + a_0}$$

then in controllable companion form

$$A = \begin{bmatrix} 0 & 1 & 0 & \dots & 0 \\ 0 & 0 & 1 & & & \\ \dots & & & \ddots & & \\ 0 & 0 & \dots & & 1 \\ -a_0 & -a_1 & & & -a_{n-1} \end{bmatrix}, B = \begin{bmatrix} 0 \\ \vdots \\ 0 \\ 1 \end{bmatrix}, C = [c_0 \dots c_{n-1}].$$

If the degree of the numerator is n-1, then we can normalize by taking the system  $G/c_{n-1}$ , then  $\overline{\sigma}(CB) = 1$ , and we may ask whether there are choices of the  $a_i$ ,  $c_i$  where this bound is attained. However, if the degree of the numerator is  $\leq n-2$ , then always CB = 0, so here the lower bound is never attained.

This leaves now two situations. In case  $\overline{\sigma}(CB) = 0$  one may wonder under what conditions  $\mathcal{K}(G) = \mathcal{M}_0(G) > 0$  is satisfied, and whether this holds under normality of A. On the other hand, when  $\overline{\sigma}(CB) > 0$  one may ask under what conditions the lower bound is attained, whether attainment  $\overline{\sigma}(CB) = \mathcal{K}(G)$  implies attainment  $\overline{\sigma}(CB) = \mathcal{M}_0(G)$ , and again, whether this is linked to normality of A.

The following example shows that in the case  $\overline{\sigma}(CB) = 0$ , normality of A is no longer the correct answer.

**Example 2.** Take  $C = \begin{bmatrix} 1 \\ -1 \end{bmatrix}$ ,  $B = \begin{bmatrix} 1 \\ -1 \end{bmatrix}$ ,  $A = \begin{bmatrix} -\lambda & 0 \\ 0 & -\mu \end{bmatrix}$  with  $0 < \lambda < \mu$ . Then  $\overline{\sigma}(CB) = 0$ , but  $Ce^{At}B = e^{-\lambda t} - e^{-\mu t} \neq 0$  for t > 0, so that  $\mathcal{M}_0(G) > 0$ , and by the Kreiss matrix theorem we also have  $\mathcal{K}(G) > 0$ . This also means that neither  $\mathcal{M}_0$  not  $\mathcal{K}$  are monotone in t. For  $\lambda = 1$ ,  $\mu = 2$  we obtain  $\mathcal{K}(G) = 0.1716 < \mathcal{M}_0(G) = 0.25$ ,

In case  $\overline{\sigma}(CB) > 0$ , the situation is also fairly unsettled, as the following examples underline.

**Example 3.** Take  $B = \begin{bmatrix} 0 & 0 & 1 \end{bmatrix}^T$ ,  $C = \begin{bmatrix} 1 & 1 & 1 \end{bmatrix}$ ,  $a_0 = 0.9608$ ,  $a_1 = 1$ ,  $a_2 = 1$ , in the controllable companion form above, which gives  $G = (s^2 + s + 1)/(s^3 + s^2 + s + 0.9608)$ , then |CB| = 1,  $\mathcal{K}(G) = \mathcal{M}_0(G) = 1$ . Here the lower bound is attained, while  $K((sI - A)^{-1}) = 1.17$ ,  $M_0((sI - A)^{-1}) = 1.43$ , thus with A not a contraction, and in particular, not normal.

**Example 4.** Now we give an example where  $\mathcal{K}(G) = \overline{\sigma}(CB) = 1$ , but  $\mathcal{K}(G) < \mathcal{M}_0(G)$ . Take A = [-q, p; 0, -q],  $B = [b_1; b_2]$ ,  $C = [c_1, c_2]$  with  $b_1c_1 + b_2c_2 = 1$ . Then with the choices q = 0.6509, p = 0.8746, C = [-19.5450, -19.1251], B = [-0.2592; 0.2126], we get  $\mathcal{K}(G) = 1 < \mathcal{M}_0(G) = 1.72$ . This situation may also arise with normal A.

**Example 5.** Example 4 can be used to analyze the special case considered in [6], where the C-matrix is  $J = [I_n, 0]$  and the B-matrix is  $J^T$ . Starting out from the system in Example 4, we have to find a regular  $2 \times 2$  matrix T such that  $CT^{-1} = [1, 0] = J$  and  $TB = [1; 0] = J^T$ . That requires  $t_{11} = c_1$ ,  $t_{12} = c_2$  and  $c_1b_1 + c_2b_2 = 1$ . Moreover, we need to fix  $t_{21}$ ,  $t_{22}$  such that  $t_{21}b_1 + t_{22}b_2 = 0$ . That gives for  $b_1 \neq 0$ :

$$T = \begin{bmatrix} c_1 & c_2 \\ -\frac{t_{22}b_2}{b_1} & t_{22} \end{bmatrix}$$

which is regular for  $t_{22} \neq 0$ . Now  $G = Ce^{At}B = CT^{-1}Te^{At}T^{-1}TB = Je^{TAT^{-1}t}J^T$ , where A is as in the previous example. Then we have  $1 = \mathcal{K}(G) < \mathcal{M}_0(G)$ , so the special structure  $C = B^T = J$  used in [6] does not help.

**Remark 4.** Reference [52] gives conditions, under which any induced system norm attains the value  $\overline{\sigma}(CB)$ . Since this applies to  $\mathcal{M}_0(G)$ , this case gives attainment.

4.3. Numerical abscissa. Hausdorff's numerical abscissa  $\omega(A)$  satisfies  $\|e^{tA}\| \leq e^{\omega(A)t}$ , hence  $e^{tA}$  is a contraction semigroup iff  $\omega(A) \leq 0$ . Since  $\omega(A) = \frac{d}{dt} \|e^{tA}\|_{t=0}^{t}$ , the slope of the curve  $t \mapsto \|e^{tA}\|$  at t=0 in the matrix case conveys global information on the entire curve, and the semigroup  $e^{tA}$ . This is why in the fluid flow literature it has been suggested that minimizing  $\omega(A_{cl})$  in closed loop might be a way to prevent transition to turbulence [24, 53, 35, 54, 55, 25]. Due to  $\omega(A) = \frac{1}{2}\overline{\lambda}(A + A^T)$  this would have the additional advantage of being an eigenvalue optimization problem, easier to handle than (9). However, in [6] we demonstrated that minimizing  $\omega(A_{cl})$  in closed loop does *not* have the desired effect of reducing transients.

Nonetheless, it is worthwhile to extend  $\omega(A)$  to systems as  $\omega(G) = \frac{d}{dt} \|Ce^{tA}B\|\Big|_{t=0}$ , because then  $\omega(G) \leq 0$  continues to be a necessary condition for attainment  $\mathcal{M}_0(G) = \overline{\sigma}(CB)$ . However, unlike the matrix case, it is no longer sufficient. Before showing this, we address necessity of attainment for the Kreiss norm:

**Proposition 3.** A necessary condition for attainment of the lower bound  $K(G) = \overline{\sigma}(CB)$  is  $\overline{\lambda}(Y + Y^T) \leq 0$ , where  $Y = Q^T C A B B^T C^T$ , and where the columns of Q form an orthonormal basis of the maximum eigenspace of  $C B B^T C^T$ .

**Proof:** Let  $A(\eta) = \frac{\eta}{2-\eta}A - I$  and put  $G(\eta, s) = C(sI - A(\eta))^{-1}B$ , then (8) can be rewritten as  $\mathcal{K}(G) = \max_{\eta \in [0,2]} \|G(\eta, \cdot)\|_{\infty}$ . Now  $\eta = 0$  contributes the value  $\overline{\sigma}(CB)$  to the maximum over  $\eta \in [0,2]$ , because A(0) = -I, and therefore  $G(0,s) = C(sI - A(0))^{-1}B = (s+1)^{-1}CB$ , hence  $\|G(0,\cdot)\|_{\infty} = \max_{\omega} |(j\omega+1)^{-1}|\overline{\sigma}(CB) = \overline{\sigma}(CB)$ , attained at the single frequency  $\omega = 0$ . In consequence, due to our hypothesis  $\mathcal{K}(G) = \overline{\sigma}(CB) > 0$ , the slope of  $\phi: \eta \mapsto \|G(\eta,\cdot)\|_{\infty}$  at  $\eta = 0$  must be non-positive, as otherwise  $\|G(\eta,\cdot)\|_{\infty} = \|C(sI - A(\eta))^{-1}B\|_{\infty}$  would attain values  $> \overline{\sigma}(CB)$  for some small  $\eta > 0$ .

To compute  $\phi'(0)$ , observe that since  $||G(0,\cdot)||_{\infty}$  is attained at the single frequency  $\omega = 0$ , we have

$$\phi'(0) = \|\cdot\|_{\infty}'(G(\eta,\cdot), \frac{d}{d\eta}G(\eta,\cdot))\Big|_{\eta=0} = \overline{\sigma}'(G(\eta,j0), \frac{d}{d\eta}G(\eta,j0))\Big|_{\eta=0}$$

$$= \overline{\sigma}'(CB, -C(A(\eta)^{-1}\frac{d}{d\eta}A(\eta)A(\eta)^{-1})B)\Big|_{\eta=0} = \overline{\sigma}'(CB, C\frac{1}{2}AB)$$

$$= \frac{1}{4}\overline{\lambda}(Q^{H}(CAB)P + P^{H}(B^{T}A^{T}C^{T})Q)$$

$$= \frac{1}{4\overline{\sigma}(CB)}\overline{\lambda}(Q^{H}C(ABB^{T} + BB^{T}A^{T})C^{T}Q),$$

where the second line uses  $\frac{d}{d\eta}\left[A(\eta)^{-1}\right] = -A(\eta)^{-1}\frac{d}{d\eta}A(\eta)A(\eta)^{-1} = -A(\eta)^{-1}\frac{2}{(2-\eta)^2}AA(\eta)^{-1}$ , which at  $\eta=0$  gives  $-\frac{1}{2}A$ , whereas the third line uses Lemma 4 based on a SVD  $G(0,0)=CB=\begin{bmatrix}Q&R\end{bmatrix}\begin{bmatrix}\overline{\sigma}(CB)I\\\Sigma\end{bmatrix}\begin{bmatrix}P^T\\T^T\end{bmatrix}$ . The last line follows by re-substituting  $Q^HCB=\overline{\sigma}(CB)P^H$ .

Note that this leads back to  $\omega(A) \leq 0$  for  $C = B = I_n$ .

**Lemma 3.** The Clarke subdifferential of the maximum singular value function is  $\partial \overline{\sigma}(G) = \{QYP^H : Y \succeq 0, \text{Tr}(Y) = 1\}$ , where  $G = \begin{bmatrix} Q & R \end{bmatrix} \begin{bmatrix} \overline{\sigma}(G) \\ \Sigma \end{bmatrix} \begin{bmatrix} P^H \\ T^H \end{bmatrix}$  is a SVD of G.

**Proof:** From  $\overline{\sigma}(G)^2 = \overline{\lambda}(GG^H)$  we get  $2\overline{\sigma}(G)\partial\overline{\sigma}(G) = F'(G)^*\partial\overline{\lambda}(F(G))$ , where  $F: \mathbb{M}^{n,m} \to \mathbb{S}^m$  is the mapping  $F(X) = XX^H$ . Now  $\partial\overline{\lambda}(GG^H) = \{QYQ^H: Y \succeq 0, \operatorname{Tr}(Y) = 1\}$ , where the columns of Q in the SVD form an orthonormal basis of the maximum eigenspace of  $GG^H$ . Furthermore,  $F'(G)D = GD^H + DG^H$ , hence for a test vector  $S \in \mathbb{S}^m$  we have by the definition of the adjoint  $\langle D, F'(G)^*S \rangle = \langle F'(G)D, S \rangle = \operatorname{Re}\operatorname{Tr} S(GD^H + DG^H) = 2\operatorname{Re}\operatorname{Tr} SDG^H = 2\operatorname{Re}\operatorname{Tr}(SG)^HD = \langle D, 2SG \rangle$ , so that the action of the adjoint is  $F'(G)^*S = 2SG$ . On substituting  $S = QYQ^H \in \partial\overline{\lambda}(GG^H)$ , we obtain  $\partial\overline{\sigma}(G) = \frac{1}{2\overline{\sigma}(G)}\{2QYQ^HG: Y\succeq 0, \operatorname{Tr}(Y) = 1\}$ . Now since  $Q^HG = \overline{\sigma}(G)P^H$  from the SVD, we obtain the claimed  $\partial\overline{\sigma}(G) = \{QYP^H: Y\succeq 0, \operatorname{Tr}(Y) = 1\}$ .

**Lemma 4.** The Clarke directional derivative is  $\overline{\sigma}'(G, D) = \frac{1}{2}\overline{\lambda}(Q^HDP + P^HD^HQ)$ .

**Proof:** We have  $\overline{\sigma}'(G,D) = \max\{\langle \Phi,D \rangle : \Phi \in \partial \overline{\sigma}(G)\} = \max\{\operatorname{Re}\operatorname{Tr}\Phi^HD : \Phi \in \partial \overline{\sigma}(G)\} = \max\{\operatorname{Re}\operatorname{Tr}PYQ^HD : Y \succeq 0, \operatorname{tr}(Y) = 1\} = \max\{\frac{1}{2}\operatorname{Re}\operatorname{Tr}Y(Q^HDP + P^HD^HQ) : Y \succeq 0, \operatorname{Tr}(Y) = 1\} = \frac{1}{2}\overline{\lambda}(Q^HDP + P^HD^HQ).$ 

On re-substituting  $Q^HG = \overline{\sigma}(G)P^H$ , we can also write this in the form  $\overline{\sigma}'(G,D) = \frac{1}{2\overline{\sigma}(G)}\overline{\lambda}(Q^HDG^HQ + Q^HGD^HQ) = \frac{1}{2\overline{\sigma}(G)}\overline{\lambda}(Q^H\left[DG^H + GD^H\right]Q)$ .

The following is now a consequence of the finite maximum rule for the subdifferential [31, Prop. 2.3.12], along with a non-smooth chain rule [31, Sect. 2.8]. A similar argument was already used in [45, Sect. III], [56, Sect. 4 and 6], and [46, Thm. 3.2].

**Lemma 5.** Suppose  $||G||_{\infty}$  is attained at the finitely many frequencies  $\omega_1, \ldots, \omega_r$ . Then  $\partial ||\cdot||_{\infty}(G) = \{\sum_{k=1}^r Q_k Y_k P_k^H : Y_k \succeq 0, \sum_{k=1}^r \operatorname{Tr}(Y_k) = 1\}$ , where for every k we let  $G(j\omega_k) = \begin{bmatrix} Q_k & R_k \end{bmatrix} \operatorname{diag}(||G||_{\infty}, \Sigma_k) \begin{bmatrix} P_k & T_k \end{bmatrix}^H$  be a SVD of  $G(j\omega_k)$ .

One also immediately gets the following description of the Clarke directional derivative of the  $H_{\infty}$ -norm:

**Lemma 6.** Suppose  $||G||_{\infty}$  is attained at the finitely many frequencies  $\omega_1, \ldots, \omega_r$ . Then  $||\cdot||'_{\infty}(G,D) = \max_{k=1,\ldots,r} \frac{1}{2}\overline{\lambda}(Q_k^H D P_k + P_k^H D^H Q_k)$ , with  $P_k, Q_k$  the same as above.

**Remark 5.** Formulas for subgradients and directional derivatives of the  $H_{\infty}$ -norm have first been given in [56, 57, 45, 46]. Using the SVD as in Lemma 3 is numerically preferable to formulas using the subdifferential  $\partial \overline{\lambda}$  directly, and we exploited this favorably in the implementation of hinfstruct and systume [58].

Corollary 1. Condition  $\overline{\lambda}(Y + Y^T) \leq 0$  is also necessary for attainment of the lower bound  $\mathcal{M}_0(G) = \overline{\sigma}(CB)$ . Moreover, when  $C = B = I_n$ , this condition is also sufficient.

**Proof:** The first part of the statement follows from (2) in tandem with Proposition 3. One may also obtain it directly by computing  $\frac{d}{dt} \|Ce^{tA}B\|\Big|_{t=0} = \overline{\sigma}'(CB,CAB) = \frac{1}{2\overline{\sigma}(CB)}\overline{\lambda}(Q^T(CABB^TC^T + CBB^TATC^T)Q) = \frac{1}{2\overline{\sigma}(CB)}\overline{\lambda}(Y + Y^T)$  using Lemma 4.

For  $C = B = I_n$  we have  $Q = I_n$ , hence  $\overline{\lambda}(Y + Y^T) = \overline{\lambda}(A + A^T) = 2\omega(A)$ , but  $\omega(A) \leq 0$  is the classical necessary and sufficient condition for a contraction semi-group.

**Example 6.** Now we show that the necessary condition  $\overline{\lambda}(Y+Y^T) \leq 0$  is generally not sufficient, which contrasts with the case  $C=B=I_n$ , where this is true. We take  $A=\begin{bmatrix}0&1\\-6&-5\end{bmatrix},\ B=\begin{bmatrix}0\\1\end{bmatrix},\ C=\begin{bmatrix}-10&1\end{bmatrix},$  where one gets  $1=\overline{\sigma}(CB)=\mathcal{K}(G)<\mathcal{M}_0(G)=1.5148,\ \omega(G)=-30$  with  $\overline{\lambda}(Y+Y^T)=-30$ , confirming that the condition is necessary for attainment of the Kreiss norm, but not sufficient for attainment of the transient amplification.

Another case is  $A = \begin{bmatrix} 0 & 1 \\ -5 & -1 \end{bmatrix}$ ,  $B = \begin{bmatrix} 0 \\ 1 \end{bmatrix}$ ,  $C = \begin{bmatrix} -8 & 1 \end{bmatrix}$ , which gives  $\overline{\sigma}(CB) = 1 < \mathcal{K}(G) = 1.13$  with  $\overline{\lambda}(Y + Y^T) = -18$ , showing that the condition is neither sufficient for attainment of the Kreiss norm, nor of transient amplification.

We do not know whether there are cases with  $\overline{\sigma}(CB) < \mathcal{K}(G) = \mathcal{M}_0(G)$ .

# 5. More system norms for transients

In this Section we consider several alternatives to the worst case peak norm and the Kreiss norm as its frequency approximation. Computability and use for optimization are primordial criteria. Persistent perturbations and noise are discussed in .

5.1.  $L^1 \to L^{\infty}$  system norm with euclidean vector norm. The discussion in Section 4.1 considers  $\mathcal{M}_0(G)$  as induced operator norm  $G: (L^1, \|\cdot\|_{1,2}) \to (L^{\infty}, \|\cdot\|_{\infty,2})$ , with the  $\ell_2$ -norm as vector norm. However, (13) shows that other choices of vector norms could lead to numerically exploitable expressions  $\mathcal{K}, \mathcal{M}$ . Choosing test vectors  $\xi \in \ell_{p'}$ ,  $\eta \in \ell_r$  gives

$$\sup_{\text{Re}(s)>0} \text{Re}(s) \|C(sI-A)^{-1}B\|_{r,p} \le \sup_{t\ge 0} \|Ce^{At}B\|_{r,p},$$

where  $||M||_{r,p}$  is the  $\ell_p \to \ell_r$  induced matrix norm. This may lead to other criteria compatible with the goal to sensing  $L^1 \to L^{\infty}$  amplification. Tractable expressions are

obtained e.g. for p = 1,  $r = \infty$ , which corresponds to taking  $\xi \in \ell_1$ ,  $\eta \in \ell_1$ . Here we get the estimate

$$\sup_{\operatorname{Re}(s)>0} \max_{ik} |c_i \operatorname{Re}(s)(sI - A)^{-1}b_k| \le \sup_{t \ge 0} \max_{ik} |c_i e^{At}b_k|$$

which reads as

$$\max_{ik} \mathcal{K}(c_i e^{A \bullet} b_k) \le \max_{ik} \mathcal{M}_0(c_i e^{A \bullet} b_k)$$

with a finite maximum of SISO Kreiss constants and transient growth norms involved. This practical entry-wise Kreiss norm offers potential to weigh some channels more than others. The upper bound of  $\mathcal{M}_0$  is again  $en \max_{ik} \mathcal{K}(c_i e^{A \cdot \bullet} b_k)$  from Theorem 2.

5.2.  $L^1 \to L^{\infty}$  system norm with  $\ell_{\infty}$ -vector norm. Now take (10), but with  $|\xi|_{\infty} \le 1$ ,  $|\eta|_{\infty} \le 1$ . We get on the right

$$|\xi^T (Ce^{At}B)\eta| \le ||(Ce^{At}B)\eta||_1 \le ||Ce^{At}B||_{1,\infty}$$

because the dual norm to  $\ell_{\infty}$  is  $\ell_1$ . However, this norm is not very helpful for matrices with large dimension m, because for  $A \in \mathbb{R}^{m \times n}$ , we have:

$$||A||_{1,\infty} = \max_{r \in \{-1,1\}^m} ||Ar||_1,$$

where  $\{-1,1\}^m$  are m-vectors of  $\pm 1$  entries. With the above technique, we easily get the following estimate

$$\max_{r \in \{-1,1\}^m} \mathcal{K}(Gr) \le \max_{r \in \{-1,1\}^m} \mathcal{M}_0(Gr).$$

5.3. Peak-to-peak norm for persistent perturbations. In this section, we discuss the choice  $p = \infty$ , q = r = 1 in Young's inequality (10), which will allow us to address the case of persistent perturbations w in (3), when for an input  $||w||_{\infty,\infty} \le 1$ , we measure the response by the same signal norm  $||G*w||_{\infty,\infty}$ . For test vectors  $\xi, \eta$  and a one-dimensional signal u we get from (10)

$$|\xi^T C(sI - A)^{-1} B \eta u(s)| \le ||e^{-st}||_{\infty} ||\xi^T C e^{At} B \eta||_1 ||u||_1 = ||\xi^T C e^{At} B \eta||_1 ||u||_1.$$

Letting the scalar signal u(t) of unit  $L_1$ -norm approach the  $\delta$ -distribution, we get

$$|\xi^T C(sI - A)^{-1} B \eta| \le \|\xi^T C e^{At} B \eta\|_1 = \int_0^\infty |\xi^T C e^{At} B \eta| dt.$$

Now let m be the number of outputs, p the number of inputs, and let  $g_{ik}(t)$  be the entries of the matrix  $Ce^{At}B$ , then with  $\|\xi\|_2 \leq 1$  and  $\|\eta\|_2 \leq 1$  we get

$$\int_{0}^{\infty} |\xi^{T} C e^{At} B \eta| dt = \int_{0}^{\infty} \left| \sum_{i=1}^{m} \sum_{k=1}^{p} \xi_{i} g_{ik}(t) \eta_{k} \right| dt 
\leq \sum_{i=1}^{m} |\xi_{i}| \sum_{k=1}^{p} |\eta_{k}| \int_{0}^{\infty} |g_{ik}(t)| dt 
= \sum_{i=1}^{m} |\xi_{i}| \sum_{k=1}^{p} ||g_{ik}||_{1} |\eta_{k}| 
\leq \left( \sum_{i=1}^{m} |\xi_{i}|^{2} \right)^{1/2} \left( \sum_{i=1}^{m} \left( \sum_{k=1}^{p} ||g_{ik}||_{1} |\eta_{k}| \right)^{2} \right)^{1/2} 
\leq \left( m \max_{i=1,\dots,m} \left( \sum_{k=1}^{p} ||g_{ik}||_{1} \right)^{2} \right)^{1/2} = \sqrt{m} \max_{i=1,\dots,m} \sum_{k=1}^{p} ||g_{ik}||_{1}.$$

When we recall that the time-domain peak-to-peak, or peak-gain, system norm is defined as

$$||G||_{\text{pk\_gn}} = \max_{u \neq 0} \frac{||G * u||_{\infty,\infty}}{||u||_{\infty,\infty}} = \max_{i=1,\dots,m} \sum_{j=1}^{p} ||g_{ij}(t)||_{1},$$

then we have shown the estimate  $||G||_{\infty} \leq \sqrt{m} ||G||_{\mathrm{pk\_gn}}$  for a system G with m outputs. The estimate remains true for more general systems with  $g_{ik} \in L^1([0,\infty),\mathbb{R}^n)$ , and even for  $(m \times p)$ -valued Radon measures, allowing to include the case of direct transmissions. In the matrix case  $||\cdot||_{\mathrm{pk\_gn}}$  reduces to the maximum row sum norm, i.e. the induced matrix norm  $\ell_{\infty} - \ell_{\infty}$ .

Let us now look at the reverse estimate, which is analogous to the right-hand estimate in the Kreiss matrix theorem (Theorem 2). Consider a stable finite-dimensional strictly proper system.

$$G: \begin{cases} \dot{x} = Ax + Bu \\ y = Cx \end{cases}$$

where  $G(t) = Ce^{At}B$ . Let  $g_{ij}(t) = c_i e^{At}b_j$ , where  $c_i$  is the ith row of C,  $b_j$  the jth column of B, then  $\|G\|_{\mathrm{pk\_gn}} = \max_{i=1,\dots,m} \sum_{j=1}^p \|g_{ij}\|_1 = \sum_{j=1}^p \|c_i e^{At}b_j\|_1$  for some i. We now relate the peak-gain norm to the Hankel singular values of G. The following

We now relate the peak-gain norm to the Hankel singular values of G. The following was proved in the SISO case p = m = 1 in [59, Thm. 2] for discrete systems, and in [60, pp. 11-12] for continuous SISO systems, where in the latter reference the idea of proof is attributed to I. Gohberg.

**Lemma 7.** Let G be real-rational, strictly proper and stable, with p outputs and McMillan degree n. Then

$$||G||_{\text{pk gn}} \le 2p^{1/2} \left(\sigma_{H1} + \dots + \sigma_{Hn}\right),$$
 (15)

where  $\sigma_{Hi}$  are the Hankel singular values of G. In particular,  $||G||_{pk_gn} \leq 2np^{1/2}||G||_{\infty}$ .

**Proof:** We have for the  $i \in \{1, ..., m\}$  where the maximum is attained

$$\begin{split} \|G\|_{\mathrm{pk\_gn}} &= \sum_{j=1}^{p} \|c_{i}e^{At}b_{j}\|_{1} = 2\sum_{j=1}^{p} \int_{0}^{\infty} \left|c_{i}e^{2A\tau}b_{j}\right| d\tau \\ &= 2\int_{0}^{\infty} \sum_{j=1}^{p} \left|\left(e^{A^{T}t}c_{i}^{T}\right)^{T}(e^{At}b_{j})\right| dt \\ &\leq 2\left(\int_{0}^{\infty} \sum_{j=1}^{p} \left\|e^{A^{T}t}c_{i}^{T}\right\|_{2}^{2}dt\right)^{1/2} \left(\int_{0}^{\infty} \sum_{j=1}^{p} \left\|e^{At}b_{j}\right\|_{2}^{2}dt\right)^{1/2} \\ &= 2p^{1/2} \left(\int_{0}^{\infty} \mathrm{Tr}(e^{A^{T}t}c_{i}^{T}c_{i}e^{At})dt\right)^{1/2} \left(\int_{0}^{\infty} \sum_{j=1}^{p} \mathrm{Tr}(e^{At}b_{j}b_{j}^{T}e^{A^{T}t})dt\right)^{1/2} \\ &= 2p^{1/2} \left(\int_{0}^{\infty} \mathrm{Tr}(e^{A^{T}t}c_{i}^{T}c_{i}e^{At})dt\right)^{1/2} \left(\int_{0}^{\infty} \mathrm{Tr}(e^{At}BB^{T}e^{A^{T}t})dt\right)^{1/2}. \end{split}$$

Recall that the observability and controllability Gramians of the system G are

$$W_o = \int_0^\infty e^{A^T t} C^T C e^{At} dt, \quad W_c = \int_0^\infty e^{At} B B^T e^{A^T t} dt.$$

Now  $\operatorname{Tr} \int_0^\infty e^{A^T t} c_i^T c_i e^{At} dt \leq \operatorname{Tr} \int_0^\infty e^{A^T t} C^T C e^{At} dt$  follows from  $c_i^T c_i \leq C^T C$  by applying a congruence transformation with  $e^{At}$ . Hence  $\|G\|_{\operatorname{pk\_gn}} \leq 2p^{1/2} \left[\operatorname{Tr}(W_o)\operatorname{Tr}(W_c)\right]^{1/2}$ . Now if we take a balanced realization, then  $W_o = W_c = \operatorname{diag}(\sigma_{H1}, \ldots, \sigma_{Hn})$  for the Hankel

singular values  $\sigma_{H_1} \ge \cdots \ge \sigma_{H_n}$ , hence  $||G||_{\text{pk\_gn}} \le 2\sqrt{p}(\sigma_{H_1} + \cdots + \sigma_{H_n}) \le 2p^{1/2}n\sigma_{H_1} \le 2p^{1/2}n||G||_{\infty}$  for a system without direct transmission. This uses  $\sigma_{H_1} \le ||G||_{\infty}$ .

Note, however, that by the Enns-Glover bound we have

$$||G||_{\infty} \ge \max{\{\overline{\sigma}(D), \sigma_{H1}\}}$$

for the maximum Hankel singular value  $\sigma_{H1}$  of G = (A, B, C, D), so our estimate holds also for systems with direct transmission. Indeed, if we define the Hankel semi-norm of a system G as

$$||G||_H = \sup \left\{ \frac{||G * u||_{L^2(T,\infty)}}{||u||_{L^2[0,T]}} : T > 0, u \in L^2[0,\infty) \right\},$$

then  $||G||_H = \sigma_{H1}$  for the maximum Hankel singular value. But with this formulation, it is immediate that  $||G||_H \leq ||G||_{\infty}$ , when we recall that  $||G||_{\infty}$  is the  $L^2$ -operator norm.

Therefore we get for a system with direct transmission

$$\|G\|_{\mathrm{pk\_gn}} \leq \|G - D\|_{\mathrm{pk\_gn}} + \|D\|_{\infty} \leq 2p^{1/2}n\sigma_{H1} + p^{1/2}\overline{\sigma}(D) \leq (2n+1)p^{1/2}\|G\|_{\infty}$$

using the fact that  $\sigma_{H1} \leq \|G\|_{\infty}$  and  $\overline{\sigma}(D) \leq \|G\|_{\infty}$ . Here  $\|D\|_{\infty}$  is the maximum row sum norm  $\max_i \sum_j |d_{ij}|$ , which is the  $\ell_{\infty} - \ell_{\infty}$  induced matrix norm satisfying  $\|D\|_{\infty} \leq p^{1/2}\overline{\sigma}(D)$ . Altogether, we have proved the following estimates for the  $H_{\infty}$ - and peak-gain norms stated in [61]:

**Theorem 3.** Let G be a stable real-rational system with n poles, p inputs and m outputs. Then

$$m^{-1/2} \|G\|_{\infty} \le \|G\|_{\mathrm{pk\_gn}} \le (2n+1)p^{1/2} \|G\|_{\infty}.$$

A large variety of synthesis experiments based on the peak-gain norm  $||G||_{pk_{gn}}$  has been presented in [61], so that our experiments here may focus on  $L_1$ -disturbances.

5.4. Noise as perturbation. In this section we consider the case  $w \in L^2$ ,  $G * w \in L^{\infty}$ , where we can rely on [30]. Consider for instance  $||G||_{(\infty,2)(2,2)} = \lambda_{\max}(CQC^T)$ , where  $Q \succeq 0$  is the unique solution of the Lyapunov equation  $AQ + QA^T + BB^T = 0$ . This norm can be optimized directly using a technique similar to [62].

## ORGANIZATION OF THE APPLICATIONS

In the following, we present applications illustrating the use of the Kreiss system norm for both analysis and feedback control design. The methods are general and can be applied to a wide range of nonlinear controlled systems. It should be emphasized that in all tests the results are certified a posteriori, since Kreiss norm optimization itself relies on a heuristic. The material is organized as follows:

**Section 6:** Kreiss norm minimization is applied to control nonlinear dynamics with periodic orbits:

- a two-dimensional limit cycle (Section 6.1),
- a four-dimensional periodic orbit (Section 6.2).

Section 7: Nonlinear regimes in the Lorenz model are considered, including chaotic (Section 7.1) and fixed points dynamics (Section 7.2). These are investigated using:

- the QC approach (Sections 7.1.1, 7.2.1),
- Kreiss norm minimization (Sections 7.1.2, 7.2.2).

### 6. Applications to nonlinear dynamics with periodic orbit attractors

6.1. Study of 2nd-order dynamics with limit cycle attractor. We start with the model of Brunton and Noack [63], which is a low-order illustration of a dynamic mechanisms known in oscillator flow, observed for instance on a larger scale in Navier-Stokes equations, see also [4]. Examples of this type include fluid flow around a cavity or a cylinder [64, 65]. The model is of the form

$$\begin{cases}
\dot{x} = \begin{bmatrix} \sigma_u & -\omega_u \\ \omega_u & \sigma_u \end{bmatrix} x + B_w w + Bu, & x \in \mathbb{R}^n, & n = 2 \\
w = \phi(x) & , \\
y = Cx
\end{cases} , (16)$$

with  $B_w := I$ ,  $B := [0 \ g]^T \ C := [0 \ 1]$ ,

$$\phi(x) := \alpha_u ||x||^2 \begin{bmatrix} -\beta_u & -\gamma_u \\ \gamma_u & -\beta_u \end{bmatrix} x ,$$

and  $\alpha_u, \beta_u > 0$ . Signals u and y are control input and measured output, respectively. It is easy to verify that the triple (A, B, C) is stabilizable and detectable.

Unlike transitional amplifier flows, oscillator flows are characterized by an unstable fixed point at the origin and a globally attractive limit cycle, here with radius  $\sqrt{\sigma_u/\alpha_u\beta_u}$ . This is shown in Fig. 1 for two initial conditions inside and outside the asymptotic limit cycle for data  $\alpha_u = 1$ ,  $\beta_u = 1$ ,  $\omega_u = 1$ ,  $\gamma_u = 0$ ,  $\sigma_u = 0.1$  and g = 1.

The goal is to compute a feedback controller u = K(s)y with two main design requirements. Firstly, K has to stabilize the origin, often called the base flow. Secondly, trajectories trapped in the limit cycle should be driven back to the origin with limited oscillations. Additional insight into this model in terms of fluid flow interpretation can be found in [63].

In order to mitigate the effects of nonlinearity, we minimize the Kreiss system norm in closed loop. This leads to the following min-max constrained program

minimize 
$$\max_{\delta \in [-1,1]} \left\| J^T \left( sI - \left( \frac{1-\delta}{1+\delta} A_{cl}(K) - I \right) \right)^{-1} J \right\|_{\infty}$$
subject to  $K$  robustly stabilizing,  $K \in \mathcal{K}$ 
$$\alpha(A_{cl}(K)) \le -\eta$$
$$\|W(s)GK(I + GK)^{-1}\|_{\infty} \le 1.$$
 (17)

Here  $K \in \mathcal{K}$  means that the controller has a prescribed structure, which could be a PID, observed-based or low-order controller, a decentralized controller, as well as any control architecture assembling simple control components. The robust stability constraint on K in (17) demands stability of the entire set of matrices  $\left\{\frac{1-\delta}{1+\delta}A_{cl} - I : \delta \in [-1,1]\right\}$ , and in particular, for  $\delta = 0$  that of  $A_{cl}(K)$ . Matrix J is a restriction matrix to the space of physical plant states since transient amplification of controller states is not relevant. We have  $J := I_n$  with n the plant state dimension for a static feedback controller and  $J := [I_n, 0_{n \times n_K}]^T$  for an  $n_K$ -order output-feedback controller (see also example 5). In terms of dimension, we have n = 2,  $n_K = 3$  when K is a 3rd-order controller,  $p_z = 2$  since z = x,  $m_w = 2$  for  $w = \phi(z)$ , and p = m = 1. The overall state dimension is therefore  $N = n + n_K + n_W = 7$  in closed loop for a 3rd-order controller and 2nd-order filter W. The latter is used to weigh the noise to measurement transfer  $T := GK(I + GK)^{-1}$ .

The notation  $\alpha(\cdot)$  refers to the spectral abscissa, and the constraint  $\alpha(A_{cl}) \leq -\eta$  in (17) therefore imposes a convergence rate to the origin for the linear dynamics in closed loop. In our experiments we have chosen  $\eta = 0.1$ .

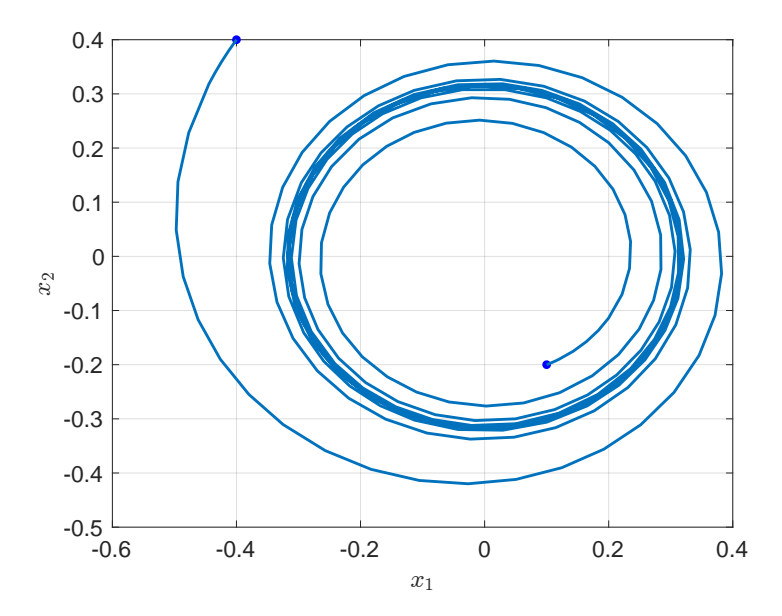


FIGURE 1. Limit cycle attractor of Brunton and Noack model

These constraints are readily implemented from the closed-loop nonlinear system:

$$\dot{x}_{cl} = A_{cl}x_{cl} + B_{w,cl}\phi_{cl}(x_{cl}), \quad x_{cl} := [x^T, x_K^T]^T, \tag{18}$$

where

$$A_{cl} := \begin{bmatrix} A + BD_K C & BC_K \\ B_K C & A_K \end{bmatrix}, \ \phi_{cl}(x_{cl}) := \phi(x), \ B_{w,cl} := J = [I_2, 0_{2 \times n_K}]^T, \tag{19}$$

and where the controller dynamics are

$$\begin{cases} \dot{x}_K = A_K x_K + B_K y, & x_K \in \mathbb{R}^{n_K} \\ u = C_K x_K + D_K y \end{cases}$$
 (20)

We exclude high-gain feedback in the high-frequency range by adding a constraint on the complementary sensitivity function  $||WT||_{\infty} \le 1$ , where W is a high-pass weighting filter  $W(s) := (1e06s^2 + 1e04s + 24.99)/(s^2 + 10000s + 2.5e07)$ .

Program (17) was solved for controller orders: 0, 1 and 3. All controllers achieve nearly the same Kreiss norm of 1.005, but differ in terms of the remaining performance/robustness constraints. This is seen by plotting transient amplifications versus time in Fig. 2. Peak values  $\mathcal{M}_0(J^T(sI-A_{cl})^{-1}J)$  are all close to 1.10 with  $||J^TJ|| = 1$  as lower bound, see Proposition 2.

The static controller K=-0.20 gives a spectral abscissa of  $\alpha(A_{cl})=-1.9899e-04$  with badly damped modes and a strong roll-off violation of  $||WT||_{\infty}=20.03$ . The 1st-order controller K(s)=(0.001071s-2.247)/(s+1.483) meets the roll-off constraint and achieves a decay rate constraints  $\alpha(A_{cl})=-0.393$ . As expected, the 3rd-order controller  $K(s)=(-0.008068s^3-6.391s^2+83.2s-1673)/(s^3+27.97s^2+252.8s+1333)$  provides the best results in terms of decay rate  $\alpha(A_{cl})=-0.811$ .

Simulations in closed loop for identical initial conditions are given in Fig. 3. Controllers are switched on at t=50 seconds when the limit cycle is well engaged. The static controller leads to a spiral trajectory barely converging to the origin, a stint which is overcome by increasing the controller order.

Global stability of the origin is established in appendix A.

6.2. Study of fourth-order dynamics with 4D periodic orbit attractor. The fourth-order model of Brunton and Noack is described as

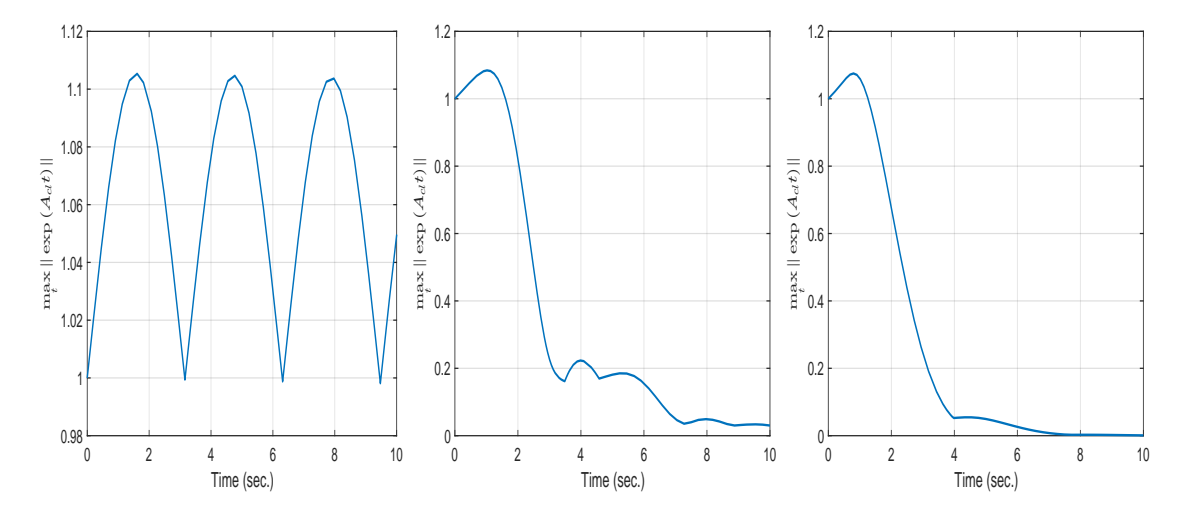


FIGURE 2. From left to right, time evolution of transient amplification for static, 1st-order and 3rd-order controller

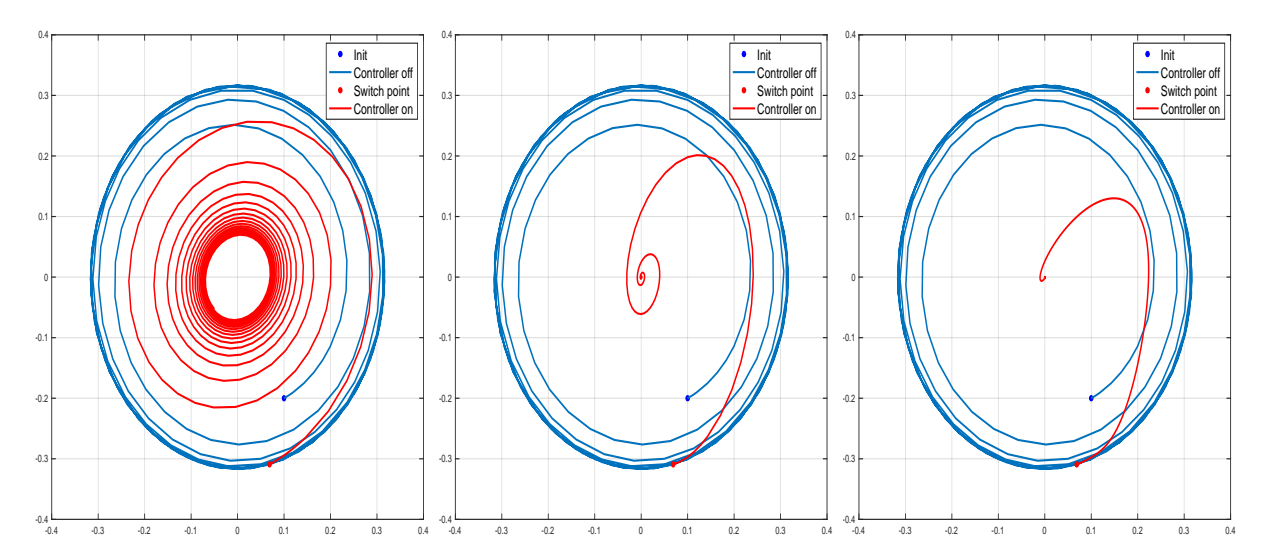


FIGURE 3. From left to right, closed-loop free responses for static, 1st-order and 3rd-order controller

$$\begin{cases} \dot{x} = Ax + B_w w + Bu, & x \in \mathbb{R}^n, \ n = 4 \\ w = \phi(x) & , \\ y = Cx \end{cases}$$
(21)

with

$$\phi(x) := (\alpha_u(x_1^2 + x_2^2)A_5 + \alpha_a(x_3^2 + x_4^2)A_6))x$$

where

$$A := \operatorname{diag}\left(\begin{bmatrix} \sigma_u & -\omega_u \\ \omega_u & \sigma_u \end{bmatrix}, \begin{bmatrix} \sigma_a & -\omega_a \\ \omega_a & \sigma_a \end{bmatrix}\right), \ B_w := I, \ B := \begin{bmatrix} 0 \ g \ 0 \ g \end{bmatrix}^T, \ C := \begin{bmatrix} 1 \ 0 \ 1 \ 0 \end{bmatrix},$$

$$A_5 := \operatorname{diag} \left( \begin{bmatrix} -\beta_{uu} & -\gamma_{uu} \\ \gamma_{uu} & -\beta_{uu} \end{bmatrix}, \begin{bmatrix} -\beta_{au} & -\gamma_{au} \\ \gamma_{au} & -\beta_{au} \end{bmatrix} \right), \ A_6 := \operatorname{diag} \left( \begin{bmatrix} -\beta_{ua} & -\gamma_{ua} \\ \gamma_{ua} & -\beta_{ua} \end{bmatrix}, \begin{bmatrix} -\beta_{aa} & -\gamma_{aa} \\ \gamma_{aa} & -\beta_{aa} \end{bmatrix} \right),$$

with data given in [63]. In this application, we have n=4,  $n_K=1$  for a 1st-order controller,  $p_z=4$  since z=x,  $m_w=4$  for  $w=\phi(z)$ , and p=m=1. The overall state dimension is therefore  $n+n_K+n_W=4+1+2=7$  for a 2nd-order filter W.

The open-loop dynamics are characterized by an unstable fixed point at the origin and an attractive 4D periodic orbit. A 1st-order controller is computed to minimize the Kreiss norm as in program (17). The roll-off filter W is unchanged. The optimal controller K(s) := (0.03538s - 0.5306)/(s + 0.667) achieves a Kreiss norm of 1.004 with decay rate and roll-off constraints all met.

Despite the apparent complexity of the dynamics, experience shows that it is possible to bring points of the periodic orbit back to the origin with a fairly large class of linear controllers. As an instance, a controller designed using a mixed-sensitivity approach [66, p. 141] with weight  $W_1 := \frac{0.001s+5}{s+0.05}$  for S and W as above for T also drives points from the periodic orbit to the origin. A 1st-order controller of this type was obtained as K(s) := (34.31s+168.1)/(s+32.47) with a closed-loop Kreiss constant of 1.54. Simulations show that closed-loop trajectories undergo large deviations before heading back to the origin. See Fig. 4. This remains risky, as attractors when still present may capture trajectories. The controller based on the Kreiss norm corrects such undesirable transients as corroborated in Figs. 4 and 5, where worst-case transients have been plotted. Finally, all controllers globally stabilize the origin and this can be established as was done for the 2nd-order system in appendix A.

## 7. APPLICATIONS TO NONLINEAR DYNAMICS WITH CHAOS AND FIXED POINTS

In this section, we consider suppression of undesirable nonlinear regimes such as chaos and fixed points for the Lorenz model.

7.1. Study of the Lorenz system with chaotic attractor. The Lorenz system [67] has three coupled first-order nonlinear differential equations

$$\begin{cases} \dot{x}_1 = p(x_2 - x_1) \\ \dot{x}_2 = Rx_1 - x_2 - x_1 x_3 \\ \dot{x}_3 = -bx_3 + x_1 x_2 , \end{cases}$$
 (22)

where p, R, and b are given parameters. In this study, we will use p = 10 and b = 1, while R will be varied to illustrate different nonlinear asymptotic regimes. To begin with, we take R = 28, where the Lorenz model has three unstable fixed points with coordinates

$$(0,0,0), (\sqrt{R-1},\sqrt{R-1},R-1), (-\sqrt{R-1},-\sqrt{R-1},R-1).$$
 (23)

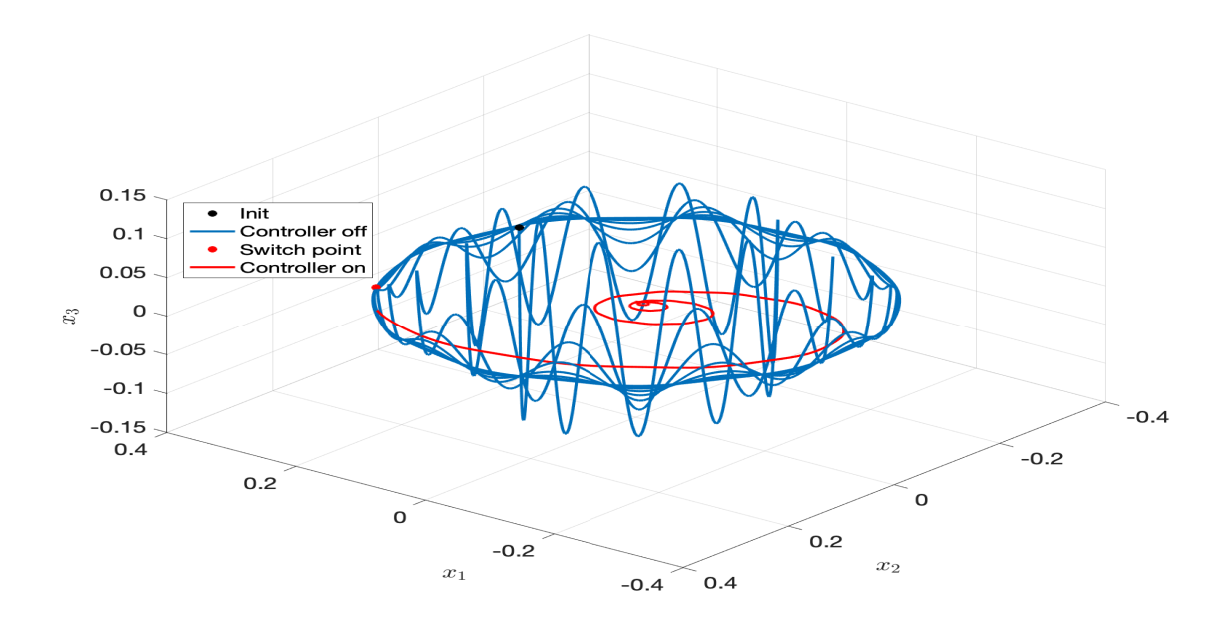
For any initial condition  $x(0) = x_0$ , a repelling effect of these fixed points is observed and trajectories are quickly captured by a chaotic attractor of double-scroll type, shown in Fig. 6.

Our feedback goal is therefore suppression of the chaotic attractor and stabilization of the origin through various feedback control strategies. We complement (22) by adding actuation and sensing, letting  $B = [0, 1, 0]^T$  and discussing several cases C, where (A, B, C) is stabilizable and detectable. The Lorenz model is then rewritten as

$$\begin{cases} \dot{x} = Ax + B_w w + Bu, & x \in \mathbb{R}^n, \ n = 3 \\ w = \phi(x) \\ y = Cx, \end{cases}$$
(24)

where u is the control input, y the measurement output. Matrix A collects the linear terms in (22),  $\phi(x) := [-x_1x_3, x_1x_2]^T$  the nonlinearity, and  $B_w := [0_{2\times 1}, I_2]^T$ . As observed before, the origin is unstable in the absence of feedback.

In this example, n = 3,  $p_z = 3$  since z = x,  $m_w = 2$  for  $w = \phi(z)$  and m = 1. The number of measurements p depends on the control strategy used. We get p = 1 when a



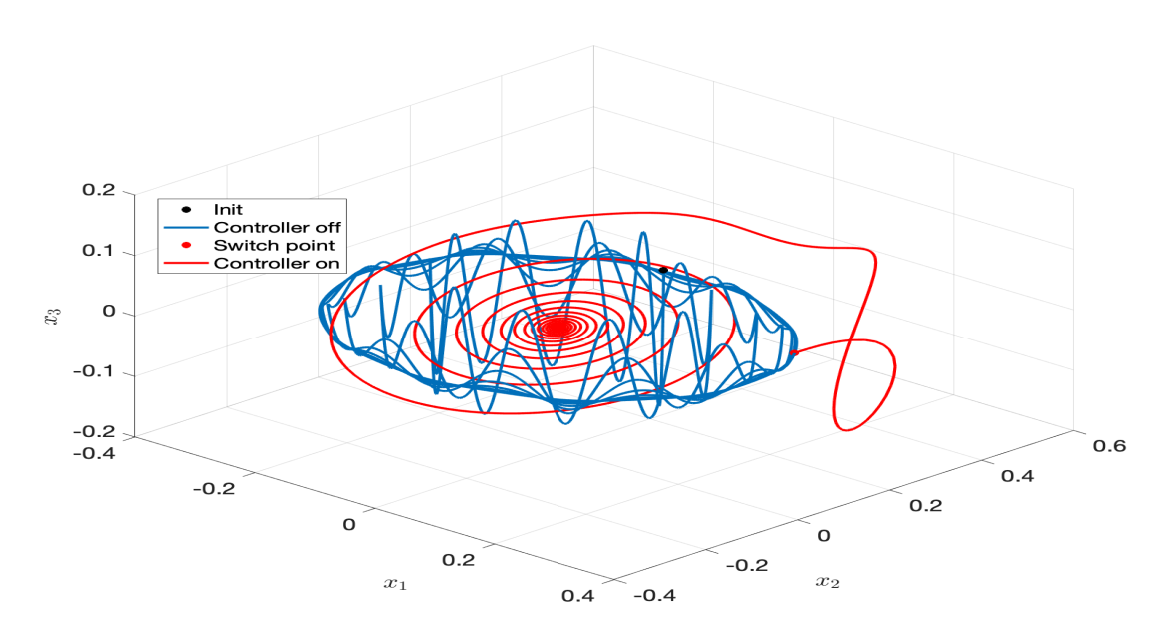


FIGURE 4. Brunton and Noack model. Free open- and closed-loop responses projected in  $(x_1, x_2, x_3)$ -space with 1st-order controllers. Top: Kreiss controller. Bottom: mixed-sensitivity controller.

single measurement is used and p=3 for full state measurement y=x. As before, we also investigate various controller orders  $n_K$ .

When a linear feedback controller u = K(s)y is used with

$$\begin{cases} \dot{x}_K = A_K x_K + B_K y, & x_K \in \mathbb{R}^{n_K} \\ u = C_K x_K + D_K y, \end{cases}$$
 (25)

the Lorenz model in closed loop becomes:

$$\dot{x}_{cl} = A_{cl}x_{cl} + B_{w,cl}\phi_{cl}(x_{cl}), \quad x_{cl} := [x^T, x_K^T]^T,$$
(26)

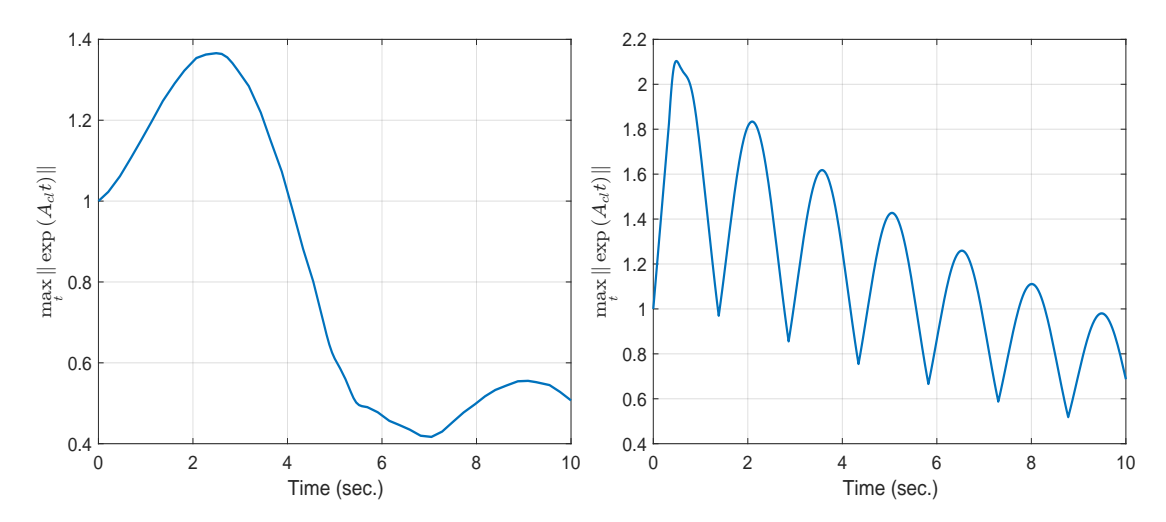


FIGURE 5. Brunton and Noack model. Transient amplifications. Left: Kreiss controller. Right: mixed-sensitivity controller.

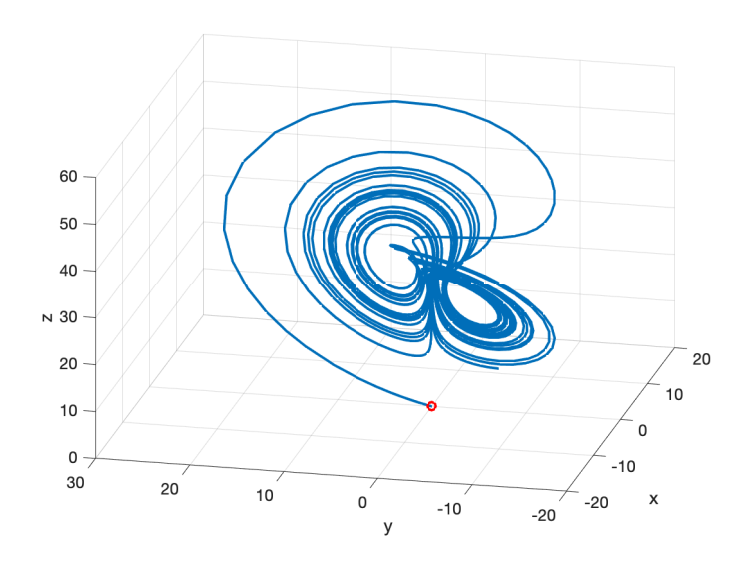


Figure 6. Double-Scroll chaotic attractor of the Lorenz model Response to state initial condition.

where

$$A_{cl} := \begin{bmatrix} A + BD_K C & BC_K \\ B_K C & A_K \end{bmatrix}, \ \phi_{cl}(x_{cl}) := \phi(x), \ B_{w,cl} := [0_{2\times 1}, I_2, 0_{2\times n_K}]^T.$$
 (27)

7.1.1. Chaos dynamics: design with the QC approach. Here we assess the stability properties of the closed loop (26) using the Lyapunov Quadratic Constraints (QC) approach of [22, 21, 68].

A particularity of the Lorenz system is the so-called *lossless property* 

$$x_{cl}^T B_{w,cl} w = 0 \text{ for all } x_{cl}, w = \phi(x),$$
(28)

which holds globally in state space. The QC approach to stability analysis now relies on the existence of a Lyapunov function  $V(x_{cl}) = x_{cl}^T X_{cl} x_{cl}$ , with  $X_{cl}$  a positive definite matrix, such that

$$\dot{V}(x_{cl}) \le -\epsilon V(x_{cl}), \epsilon > 0$$

for all  $x_{cl}$ , w such that the quadratic constraint in (28), when disregarding  $w = \phi(x)$ , holds. This is clearly a sufficient possibly conservative condition because of the chosen quadratic in  $V(x_{cl})$ , and also because the specific dependence of w on the states x is ignored. Using a S-procedure argument [21, 27] to aggregate the lossless constraint (28), this is rewritten as

$$\dot{V}(x_{cl}) + \mu_0 x_{cl}^T B_{w,cl} w \le -\epsilon V(x_{cl})$$

for all  $x_{cl}$ , w, where  $\mu_0$  is a S-procedure parameter (sometimes called a Lagrange multiplier), which here is unsigned, as the constraint (28) is an equality. The following equivalent matrix inequality constraints are obtained:

$$\begin{bmatrix} A_{cl}^T X_{cl} + X_{cl} A_{cl} + \epsilon X_{cl} & X_{cl} B_{w,cl} + \mu_0 B_{w,cl} \\ B_{w,cl}^T X_{cl} + \mu_0 B_{w,cl}^T & 0 \end{bmatrix} \leq 0, \ X_{cl} \succ 0.$$
 (29)

We have the following:

**Theorem 4.** There exist a linear time-invariant controller (25) such that the sufficient global stability conditions (29) hold, if and only if there exist solutions  $X = X^T$  and  $Y = Y^T$  in  $\mathbb{R}^{(n-n_{\phi})\times(n-n_{\phi})}$  to the following LMIs:

$$N_{C}^{T} \left( A^{T} \begin{bmatrix} X & 0 \\ 0 & I \end{bmatrix} + \begin{bmatrix} X & 0 \\ 0 & I \end{bmatrix} A + \epsilon \begin{bmatrix} X & 0 \\ 0 & I \end{bmatrix} \right) N_{C} \prec 0$$

$$N_{B}^{T} \left( A \begin{bmatrix} Y & 0 \\ 0 & I \end{bmatrix} + \begin{bmatrix} Y & 0 \\ 0 & I \end{bmatrix} A^{T} + \epsilon \begin{bmatrix} Y & 0 \\ 0 & I \end{bmatrix} \right) N_{B} \prec 0$$

$$\begin{bmatrix} X & 0 & I & 0 \\ 0 & I & 0 & I \\ I & 0 & Y & 0 \\ 0 & I & 0 & I \end{bmatrix} \succeq 0,$$

$$(30)$$

where  $N_C$  and  $N_B$  are bases of the null space of C and  $B^T$ , respectively.

Moreover, the controller order is determined by the rank of  $I_{n-n_{\phi}} - XY$  with  $n_{\phi}$  the vector dimension of the nonlinearity.

### **Proof:** See appendix B.

Note that Theorem 4 applies to any nonlinear system with similar structure for which (28) holds.

For the Lorenz model, we have a loss of rank of at least  $n_{\phi} = 2$ , the vector dimension of the nonlinearity. For the QC approach this means that controllers can have order at most  $n - n_{\phi} = 1$ . For problems with nonlinearity of dimension n, the plant order, only static output feedback controllers can be computed. In that case the BMI (38) reduces to the LMI feasibility problem:

$$(A + BKC)^T + (A + BKC) \prec 0,$$

or equivalently, to minimization of the numerical abscissa  $\omega(A+BKC)$ , defined as  $\omega(M) := 1/2\lambda_{\max}(M+M^T)$ . This is in line with the results in [21] for transitional flow studies. On the other end, when  $n_{\phi} = 0$ , the plant is linear and the controller can be of full order. The last step is construction of the controller given X and Y from (30), which is standard and found in [69].

Application to the Lorenz model with x-1-measurement, yields a 1st-order controller K(s) = -(306.5 + 2809)/(s + 0.1044). Simulation in closed loop is shown in Fig. 7 (top left corner). The feedback controller is switched on after 15 seconds, when the chaotic regime is well engaged.

Characterization of state-feedback controllers is easily derived from the second projection LMI in (30), or using u = Kx and C = I in the BMI (29):

$$(A + BK)^T \operatorname{diag}(X, I) + (.)^T \prec -\epsilon \operatorname{diag}(X, I), \ X \succ 0, \tag{31}$$

or equivalently, using a congruence transformation  $\operatorname{diag}(Y, I) = \operatorname{diag}(X, I)^{-1}$ , on the leftand right-hand sides of the first matrix inequality in (31)

$$(A + BK)\operatorname{diag}(Y, I) + (.)^{T} \prec -\epsilon\operatorname{diag}(Y, I), Y \succ 0.$$
(32)

The constraint (32) is turned into an LMI feasibility program using the standard change of variable  $V := K \operatorname{diag}(Y, I)$ :

$$A\operatorname{diag}(Y,I) + BV + (.)^T \prec -\epsilon\operatorname{diag}(Y,I), Y \succ 0.$$
(33)

All LMI characterizations derived so far can be solved by standard convex SDP software as LMILab [58] or SeDuMi [70]. Solving (33) for the Lorenz model yields a globally stabilizing state-feedback controller  $K = V \operatorname{diag}(P_{11}, I) = [-154, 400.245, 0]$ . A simulation is shown in Fig. 7 top right.

The fact that the state-feedback controller does not use the  $x_3$ -measurement suggests that even simpler controller structures should be satisfactory, e.g. using static output feedback in  $x_1$  or  $x_2$ . For  $x_1$ -measurement alone, we have C = [1,0,0] and the BMI characterization is the same as in (31) with A + BKC replacing A + BK. For a scalar K this is easily solved by sweeping an interval of K values and solving for the resulting LMIs with K fixed. We obtain K = -27.01 with search interval [-100, 100]. Simulations are displayed in Fig. 7, bottom left.

Similar results can be obtained with  $x_2$ -measurement feedback alone. The gain value is K = -27.01, and simulations are given in Fig. 7, bottom right.

7.1.2. Chaos dynamics: Kreiss norm minimization . We now investigate whether similar results can be achieved with controllers minimizing the Kreiss system norm. Here we follow a different strategy which is to decouple the linear dynamics  $\dot{x}=Ax$  from the nonlinearity  $\phi$  by way of mitigating transients due to initial conditions or  $L^1$  disturbances. While this is a heuristic in the first place, it can of course in a second step be certified rigorously using the same QC approach, now for analysis. This has the advantage that BMIs are replaced by LMIs. In addition, the technique is applicable in a much more general context beyond the Lorenz model as seen in sections 6.1 and 6.2 when the QC approach turns out too conservative.

Controllers based on minimizing the Kreiss norm alone are computed through the following min-max program

minimize 
$$\max_{\delta \in [-1,1]} \left\| J^T \left( sI - \left( \frac{1-\delta}{1+\delta} A_{cl}(K) - I \right) \right)^{-1} J \right\|_{\infty}$$
 subject to  $K$  robustly stabilizing,  $K \in \mathcal{K}$ , (34)

with the definitions already given for program (17).

Program (34) was solved for four controller structures:  $x_1$ -measurement dynamic feedback, state feedback, static  $x_1$ -measurement feedback, and  $x_2$ -measurement feedback. Controller gains were computed as K(s) = -(47.06s+715.7)/(s+17.95), [-41.07, -13.78, 0], -34.70 and -32.55, respectively. In each case a Kreiss constant of unit value with  $\mathcal{M}_0(G) = 1$  was achieved, meaning that the linear dynamics do no longer amplify transients in the Lorenz model. Note that unlike the matrix case,  $\mathcal{M}_0(G) = 1$  cannot be inferred directly from  $\mathcal{K}(G) = 1$ , but can be certified a posteriori. Naturally, all controllers have been tested for global stability of the Lorenz model, which for K fixed uses the characterization in (29) and requires solving a convex SDP. Simulations are given in Fig. 8.

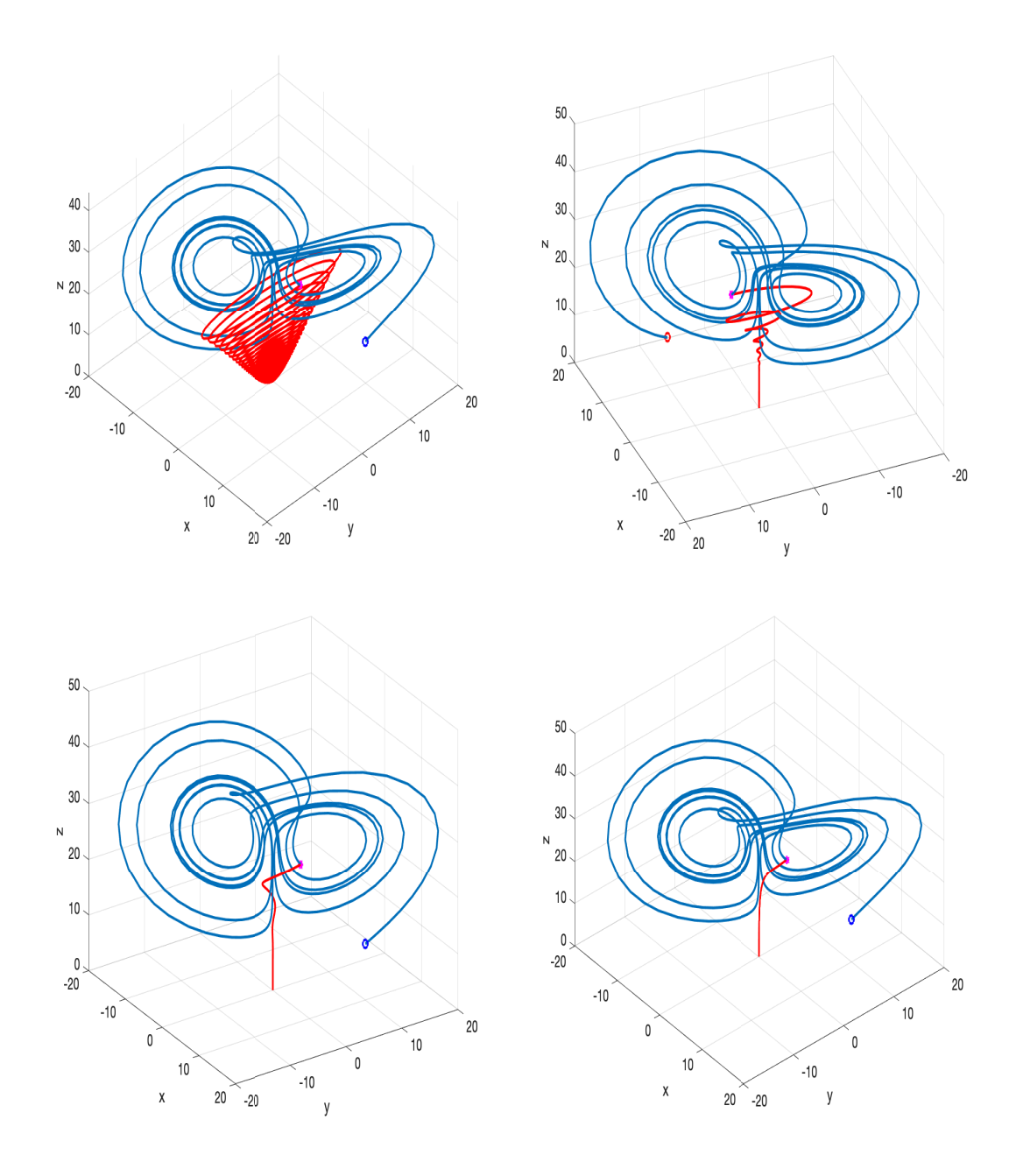


FIGURE 7. Suppression of Lorenz double-scroll chaotic attractor using QC approach
Top left:  $x_1$ -measurement dynamic feedback, Top right: state feedback
Bottom left:  $x_1$ -measurement static feedback, Bottom right:  $x_2$ -measurement static
feedback

Open loop in blue: response to state initial condition. Closed loop in red: response when controller is on.

7.2. Study of the Lorenz system with fixed points. For R < 1, the origin is the only stable equilibrium of (22) and the Lorenz model is then globally stable. When the Lorenz parameter is chosen as 1 < R < 17.5, the chaotic attractor disappears and is replaced with fixed points. For instance, when R = 10, the Lorenz model has an unstable fixed point at the origin and two stable fixed points given in (23). A typical illustration of that situation is shown in Fig. 9. Trajectories with initial conditions arbitrarily close to 0 are quickly captured by one of the fixed points.

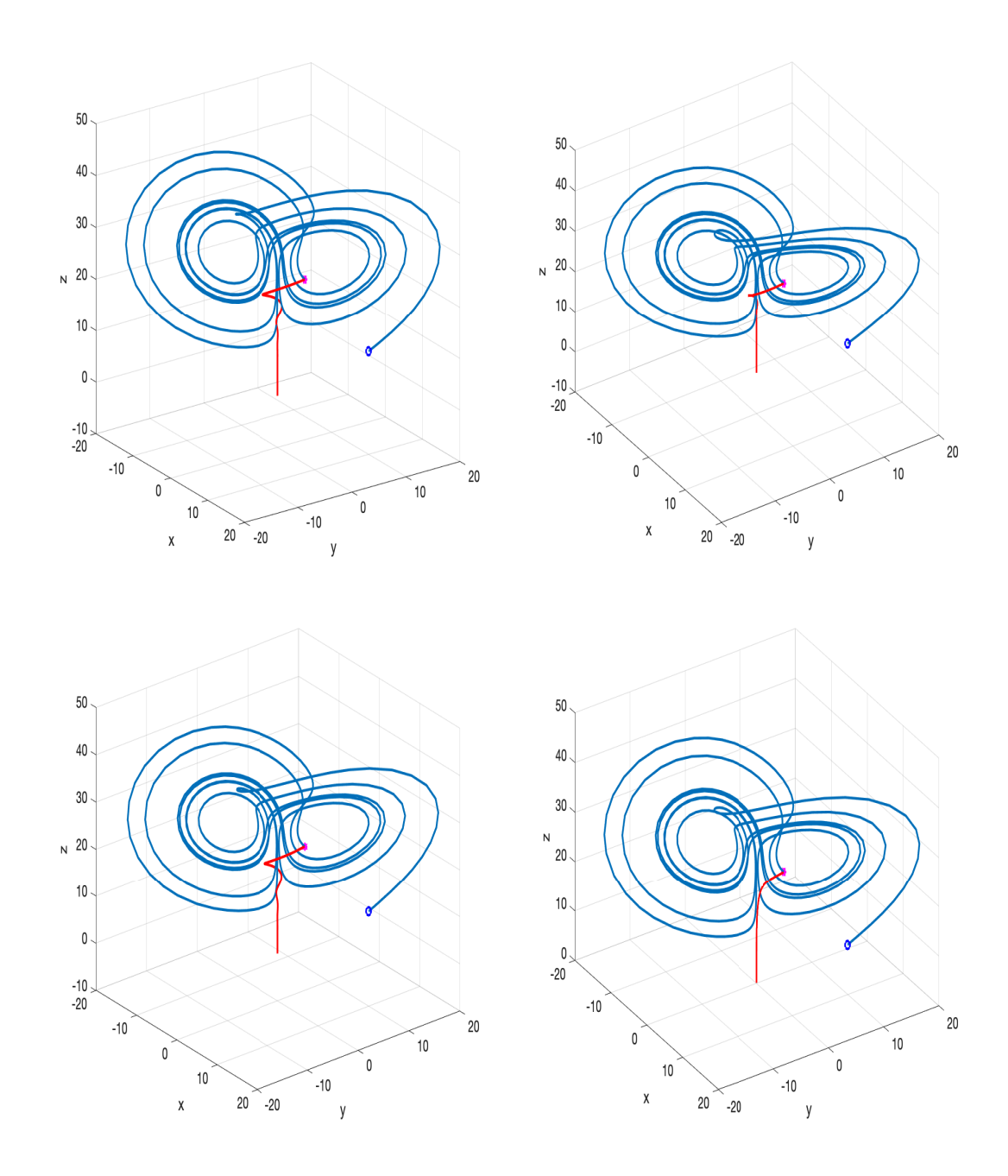


FIGURE 8. Suppression of Lorenz chaotic attractor using Kreiss norm minimization

Top left:  $x_1$ -measurement dynamic feedback, Top right: state feedback Bottom left:  $x_1$ -measurement static feedback, Bottom right: :  $x_2$ -measurement static feedback

Open loop: blue curve, Closed loop: red curve.

Despite this quite different pattern of the attracting regime, synthesis proceeds along similar lines as in section 7.1. We remove the undesirable fixed points and stabilize the origin globally using static state-feedback, and dynamic and static output-feedback, comparing QC approach and Kreiss norm minimization.

7.2.1. Fixed-point dynamics: design with the QC approach. As before, we start with the QC approach. A state-feedback controller was computed as K = [-136.40, 0.24, 0]. Again the  $x_3$  measurement is not used. That leads us to computing static output feedback

controllers given as K = -9.01 and K = -9.01 for the  $x_1$  and  $x_2$  measurements alone, respectively. A dynamic 1st-order  $x_1$ -measurement output feedback controller was computed as K = -(288.5s + 2807)/(s + 0.104) based on Theorem 4. All computed controllers globally stabilize the origin. This is illustrated in Fig. 10 for two initial conditions.

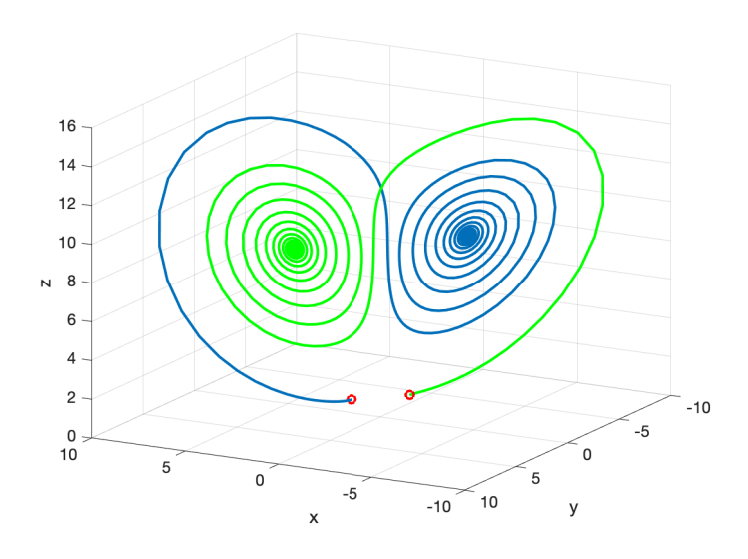


FIGURE 9. Lorenz model for 1 < R < 17.5Unstable origin and two stable fixed points

7.2.2. Fixed-point dynamics: Kreiss system norm. Controllers with identical structure were computed using Kreiss norm minimization. Dynamic 1st-order  $x_1$ -measurement output feedback, full state,  $x_1$ -measurement and  $x_2$ -measurement static feedback were obtained as K = -(12.23s + 67.63)/(s + 5.541), K = [-4.47, -6.92, 0], K = -26.32 and K = -11.53, respectively. All controllers were certified to stabilize the origin globally through feasibility of the LMI (29). Simulations are shown in Fig. 11 and should be compared to Fig. 10.

#### 8. Conclusion

The idea to stabilize nonlinear systems in closed loop by mitigating transients of the linearized closed loop was investigated, the rationale being that large transients are responsible for driving the nonlinear dynamics outside the region of local stability. Heuristic approaches tailored to transients caused by noise, persistent perturbations, and finite consumption disturbances were obtained, opening up new possibilities for analysis and control of linear and nonlinear systems.

The time-domain worst case transient peak norm  $\mathcal{M}_0(G)$  was identified as suitable to assess transients caused by  $L_1$ -disturbances. The Kreiss system norm  $\mathcal{K}(G)$  was introduced and studied as a frequency domain approximation of  $\mathcal{M}_0(G)$ , better suited for the purpose of optimization due to its representation as a parametric robust control problem. In each case the Kreiss-norm objective was effectively combined with other performance and robustness specifications as used in practice, underlining its relevance. In our numerical testing, Kreiss norm optimization was evaluated by matching it, in small to medium size cases where possible, with a properly extended QC approach.

The Kreiss norm approach is particularly effective for plants with up to several hundred states. This concerns the evaluation of Kreiss norm on the one hand, which has polynomial complexity, but also feedback design, which is naturally more challenging,

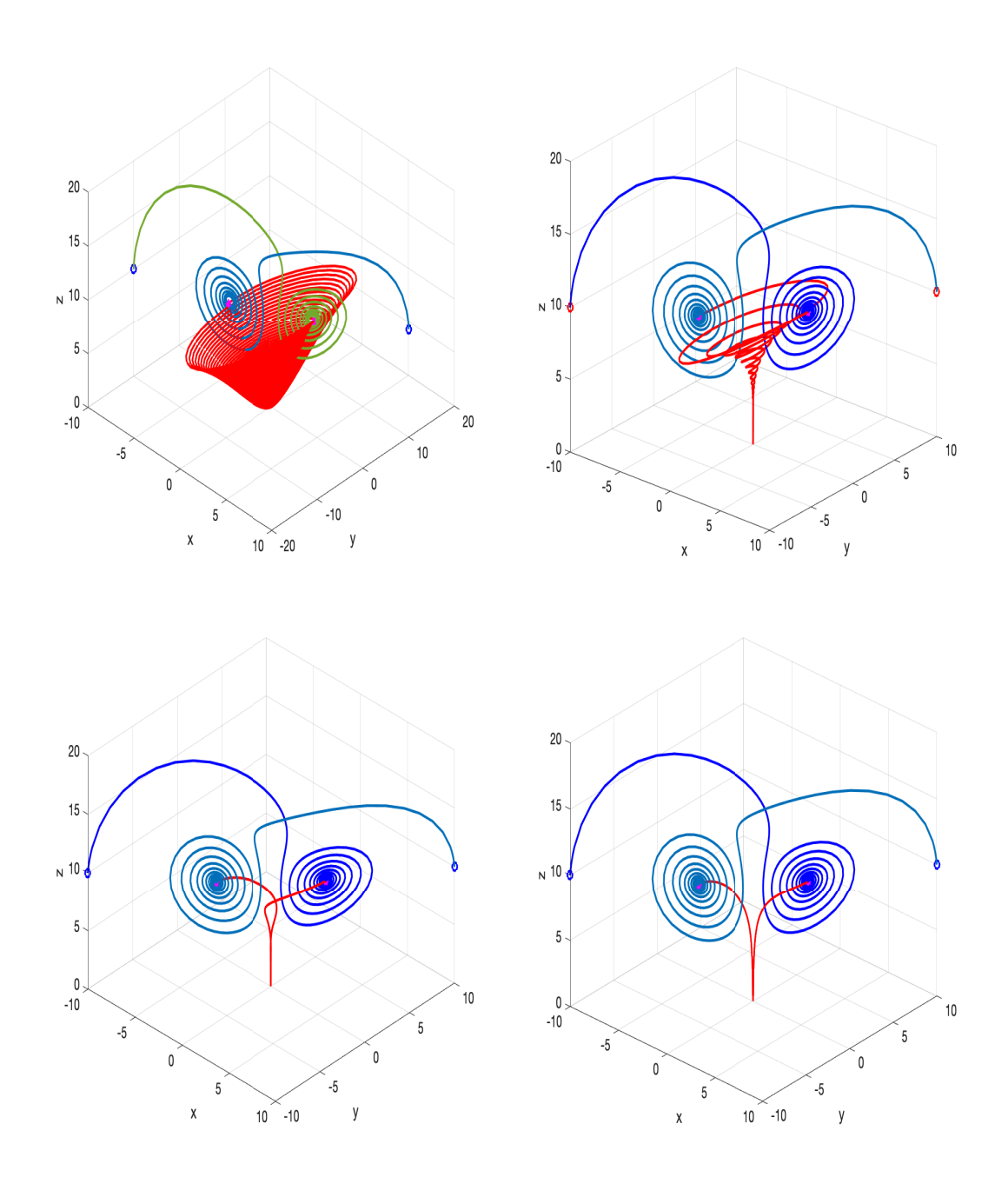


FIGURE 10. Suppression of fixed point attractors using QC approach Top left:  $x_1$ -measurement dynamic feedback, Top right: state feedback Bottom left: :  $x_1$ -measurement static feedback, Bottom right: :  $x_2$ -measurement static feedback

Open loop: blue curve. Closed loop: red curve.

but still manageable at such sizes. Future work may strive to enable Kreiss norm minimization for large-dimensional plants, such as discretizations of realistic fluid flow models or other PDE models. While challenging, this may be within reach when model sparsity is exploited and specialized linear algebra is used. In contrast, LMI techniques and SOS certificates such as seen in the application section are no longer viable options for such huge dimensions.

Over the past two years our optimizer [56, 45, 44], available through *systune* in [58], has been used regularly in industrial applications, see e.g. [71, 72, 73, 74, 75, 76, 77]. A

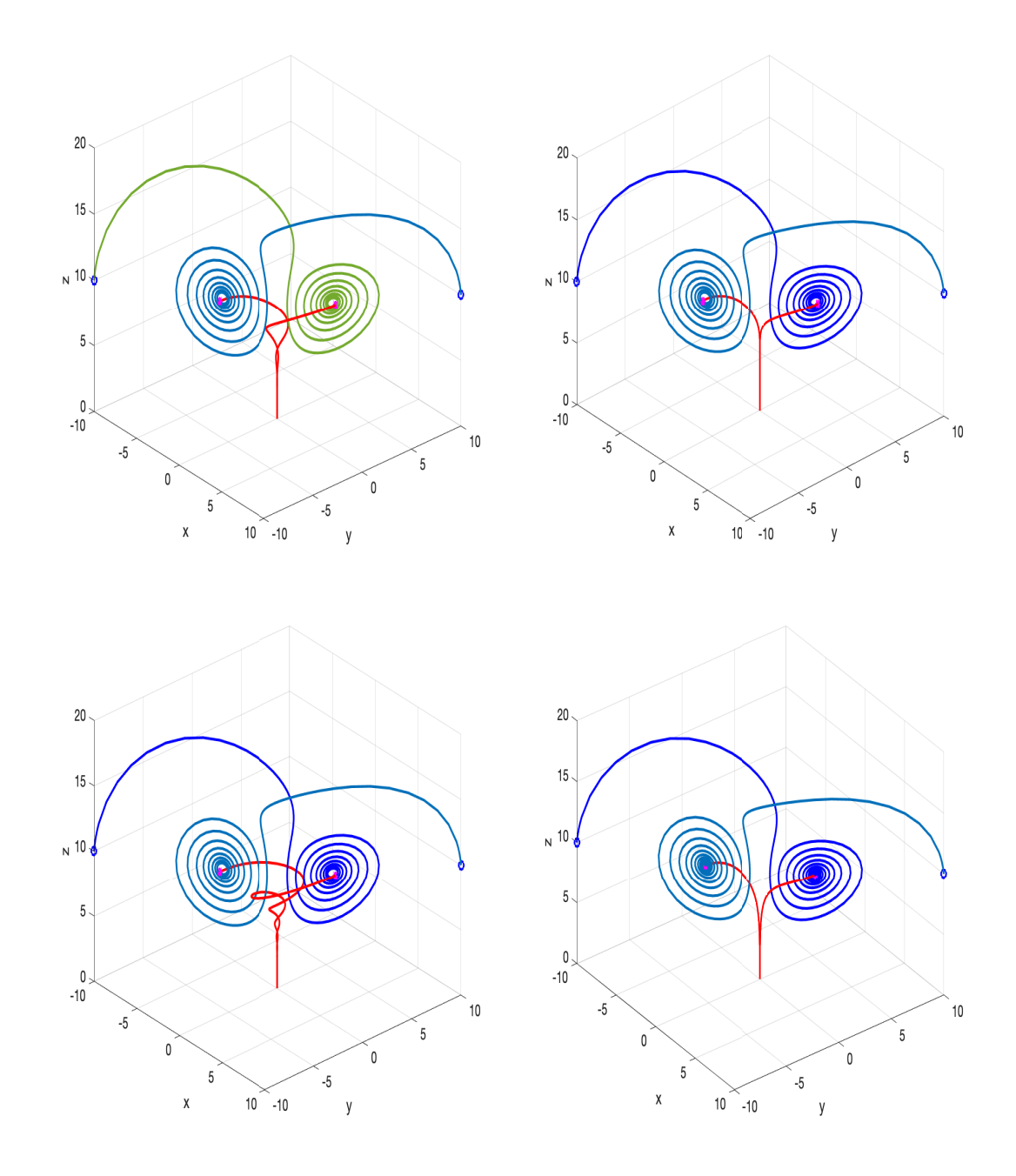


FIGURE 11. Suppression of fixed point attractors using Kreiss norm minimization Top left:  $x_1$ -measurement dynamic feedback, Top right: state feedback Bottom left: :  $x_1$ -measurement static feedback, Bottom right: :  $x_2$ -measurement static feedback Open loop: blue curve, Closed loop: red curve.

specific interest for practitioners is that it allows parametric robustness in tandem with multi-objective synthesis and controllers of designer-chosen structure.

### APPENDIX A

We consider the closed-loop system (16) in polar coordinates

$$\dot{r} = \sigma r - \alpha \beta r^3 + gKr \sin^2 \phi$$

$$\dot{\phi} = \omega + \alpha \gamma r^2 + gK \cos \phi \sin \phi$$
(35)

First observe that r(t) must be bounded. Indeed, we have  $\dot{r} \leq 0$  for

$$r^2 \ge \frac{\sigma + gK\sin^2\phi}{\alpha\beta}$$

which due to K < 0 means that states r with

$$r^2 > \frac{\sigma}{\alpha\beta} =: r_0^2$$

cannot be reached (from below). Namely if  $r(0) < r_0$ , then the trajectory may never reach values  $r(t) > r_0$ , as this would require derivatives  $\dot{r} > 0$  in between  $r_0$  and  $r(t) > r_0$ . Even when  $r(0) > r_0$ , then  $\dot{r} < 0$  on some  $[0, \epsilon)$ , so the trajectory decreases until  $r(t) = r_0$  is reached, and then the previous argument shows that it cannot rebounce to values  $> r_0$ . In conclusion, the trajectories of the system are bounded.

Let us look for steady states  $(x^*, y^*)$ . In the original (x, y)-system we have (with  $r^2 = x^2 + y^2$ )

$$0 = (\sigma - \alpha \beta r^2)x - \omega y - \alpha \gamma r^2 y$$
$$0 = \omega x + \alpha \gamma r^2 x + \sigma y - \alpha \beta r^2 y + gKy$$

and this can be written

$$A(r) := \begin{bmatrix} \sigma - \alpha \beta r^2 & -\omega - \alpha \gamma r^2 \\ \omega + \alpha \gamma r^2 & \sigma - \alpha \beta r^2 + gK \end{bmatrix} \begin{bmatrix} x \\ y \end{bmatrix} = \begin{bmatrix} 0 \\ 0 \end{bmatrix}$$

For this system to have a non-zero solution  $(x^*, y^*) \neq (0, 0)$ , the determinant of the system matrix A(r) must vanish, which leads to

$$(\sigma - \alpha \beta r^2)^2 + gK(\sigma - \alpha \beta r^2) + (\omega + \alpha \gamma r^2)^2 = 0.$$

This quadratic equation in  $\sigma - \alpha \beta r^2$  has no real solution for  $g^2 K^2 - 4(\omega + \alpha \gamma r^2)^2 < 0$ , which gives the following

**Proposition 4.** Suppose  $-K < \frac{2\omega}{g}$ . Then the only steady state of the closed-loop system is (0,0).

The origin is locally exponentially stable, so there exists a largest ball  $B(0,\rho)$  such that all trajectories starting in  $B(0,\rho)$  converge to (0,0). Suppose  $\rho < \infty$ , then there exists  $(x_0,y_0) \notin B(0,\rho)$  such that the trajectory starting at  $(x_0,y_0)$  does not enter the ball  $B(0,\rho)$ . Since it is a bounded trajectory, the Poincaré-Bendixon theorem implies that it must approach a limit cycle. For a limit cycle to exist, the system must admit a periodic solution.

We therefore look for conditions which allow to exclude the existence of a periodic solution. The Bendixon condition tells that this is the case when  $P_x + Q_y$  does not change sign, where P, Q are the right hand sides of (16) with the loop u = Ky closed. We get

$$P_x + Q_y = 2\sigma - 4\alpha\beta r^2 + gK$$

and this has negative sign for  $K < -\frac{2\sigma}{g}$ . We conclude the

**Proposition 5.** Suppose  $K \in \mathbb{R}$  satisfies  $K < -\frac{2\sigma}{g}$  and  $-K < \frac{2\omega}{g}$ . Then (16) is globally stabilized by the static controller u = Ky.

A.1. **Dynamic controllers.** Consider the case of dynamic controllers. Closed-loop dynamics are obtained as follows  $(r^2 = x^2 + y^2)$ :

$$\begin{bmatrix} \dot{x} \\ \dot{y} \\ \dot{x}_K \end{bmatrix} = \begin{bmatrix} (\sigma - \alpha\beta r^2) & -(\omega + \alpha r^2 \gamma) & 0 \\ (\omega + \alpha\gamma r^2) & (\sigma + gD_K - \alpha\beta r^2) & gC_K \\ 0 & B_K & A_K \end{bmatrix} \begin{bmatrix} x \\ y \\ x_K \end{bmatrix}.$$

The equilibrium equations give  $x_K = -A_K^{-1}B_Ky$ , assuming that  $A_K$  is invertible. This leads to

$$\begin{bmatrix} (\sigma - \alpha \beta r^2) & (\omega + \alpha r^2 \gamma) \\ (\omega + \alpha \gamma r^2) & (\sigma - \alpha \beta r^2 + g(D_K - C_K A_K^{-1} B_K)) \end{bmatrix} \begin{bmatrix} x \\ y \end{bmatrix} = \begin{bmatrix} 0 \\ 0 \end{bmatrix},$$

which as before, has (0,0) as unique solution if and only if the system matrix is invertible. The determinant quadratic equation in  $\sigma - \alpha \beta r^2$  has no real solution and is thus non-zero when

$$(g(D_K - C_K A_K^{-1} B_K))^2 - 4(\omega + \alpha \gamma r^2)^2 < 0$$

which is guaranteed when

$$|D_K - C_K A_K^{-1} B_K| < 2\omega/g.$$

Note the latter involves a constraint on the DC gain of the dynamic controller  $K(s) = C_K(sI - A_K)^{-1}B_K + D_K$ .

The polar form of these differential equations for (x, y) is obtained as

$$\dot{r} = \sigma r - \alpha \beta r^3 + g D_K r \sin^2 \phi + g C_K x_K \sin \phi$$

$$\dot{\phi} = \omega + \alpha \gamma r^2 + g D_K \cos \phi \sin \phi + g C_K x_K \cos \phi$$

$$\dot{x}_K = A_K x_K + B_K r \sin \phi$$
(36)

Assuming that  $A_K$  is Hurwitz as is the case for all controllers based on the Kreiss norm, the third equation in (36) gives us on every finite interval  $[0, t_0]$  an estimate of the form  $\max_{0 \le t \le t_0} |x_K(t)| \le c \max_{0 \le t \le t_0} r(t)$  for a constant c > 0 independent of  $t_0$ . Indeed,  $x_K(t) = \exp(tA_K)x_0 + \int_0^t \exp((s-t)A_K)B_K \sin\phi(s)r(s)ds$ , hence from Young's inequality (with  $q = r = \infty$ , p = 1), we get

$$\max_{0 \le t \le t_0} |x_K(t)| \le c_1 + ||B_K|| || \exp(tA_K)||_1 \max_{0 \le t \le t_0} r(t) \le c_1 + c_2 \max_{0 \le t \le t_0} r(t) \le c \max_{0 \le t \le t_0} r(t).$$

Therefore by the comparison theorem, (see Lemma 8 below), applied to the first equation in (36), r(t) is bounded above by the solution of the equation  $\dot{r} = (\sigma + g|D_K| + g||C_K||c)r - \alpha\beta r^3$ . The latter, however, is globally bounded, as the negative term  $-\alpha\beta r^3$  dominates for large r > 0. Having established global boundedness of r(t), we go back into the equation  $\dot{x}_K = A_K x_K + B_K r \sin \phi$ , from which we now derive global boundedness of  $x_K$ , and so altogether trajectories of (36) remain bounded.

**Lemma 8.** (See e.g. [78, Thm. 2.1, p. 93]). Suppose  $\phi$  satisfies  $|\phi(t, x) - \phi(t, x')| \leq M|x - x'|$  for all  $t \in [t_0, t_1]$  and x, x', and is jointly continuous. Let v(t) be an absolutely continuous function such that  $\dot{v}(t) \leq \phi(t, v(t))$  for almost all  $t \in [t_0, t_1]$ . Then  $v(t) \leq u(t)$  on  $[t_0, t_1]$ , where u(t) is the solution of  $\dot{u}(t) = \phi(t, u(t))$  with initial value  $u(t_0)$  satisfying  $v(t_0) \leq u(t_0)$ .

We are now in the situation addressed in [79, Corollary], which says that if a  $C^1$ -function V(x) can be found satisfying

$$\dot{V}(x) + \ddot{V}(x) \neq 0 \text{ for all } x \neq 0$$
(37)

then trajectories either converge  $x(t) \to 0$ , or escape to infinity  $|x(t)| \to \infty$ . Since we have already ruled out the latter, we have then a certificate of global asymptotic stability. For this model, we have used the more restrictive condition  $\dot{V}(x) < 0$ , with

 $V(x) = V_1(x) + \dot{V}_2(x)$  and  $V_1$ ,  $V_2$  are chosen as multivariate polynomials. See [80] for details. The polynomials are then sought using *sostools* [81].

For both the 1st- and 3rd-order controllers, a solution was obtained with  $V_1$  and  $V_2$  sums of monomials of degree 2. For the simpler 1st-order controller, with  $x_{cl} = (x, y, x_K)$  this reads

$$V_1(x_{cl}) = 2.556x^2 - 1.389xy - 0.02803xx_K + 2.897y^2 - 3.846e - 5yx_K + 0.003159x_K^2$$
 
$$V_2(x_{cl}) = -0.2061x^2 + 0.008941xy - 1.324e - 6xx_K - 0.1787y^2 + 1.641e - 5yx_K - 0.008169x_K^2 \,.$$
 We have established that  $x(t) \to 0$ .

## Appendix B

Since the first matrix in (29) has a zero principal sub-matrix, the corresponding row and column terms should be zero for this matrix to be negative semi-definite. This leads to  $X_{cl}B_{w,cl} + \mu_0 B_{w,cl} = 0$ . Also, the (1, 1) sub-matrix should be negative semi-definite. Using a partitioning in  $X_{cl}$  conformable to that of  $B_{w,cl}$  in (27), we have

$$X_{cl} = \begin{bmatrix} X & X_{12} & X_{13} \\ X_{12}^T & X_{22} & X_{23} \\ X_{13}^T & X_{23}^T & X_{33} \end{bmatrix}, \text{ with } X \in \mathbb{R}^{(n-n_{\phi})\times(n-n_{\phi})}, X_{22} \in \mathbb{R}^{n_{\phi}\times n_{\phi}}, X_{33} \in \mathbb{R}^{n_{K}\times n_{K}}$$

with  $n_{\phi}$  the vector dimension of the nonlinearity  $\phi$ . This gives  $X_{12} = 0$ ,  $X_{22} = -\mu_0 I$  and  $X_{23} = 0$ . Due to homogeneity of the problem,  $\mu_0$  is set to -1, and since  $X_{22}$  should be positive definite, we get  $X_{22} = I$ . Also, non-strict feasibility can be replaced with strict feasibility by reducing  $\epsilon$  if necessary. Summing up, assessing global stabilization with a dynamic controller K(s) reduces to a specially structured Lyapunov inequality

$$A_{cl}^{T}X_{cl} + X_{cl}A_{cl} + \epsilon X_{cl} \prec 0, \quad X_{cl} = \begin{bmatrix} X & 0 & X_{13} \\ 0 & I & 0 \\ X_{13}^{T} & 0 & X_{33} \end{bmatrix}, X_{cl} \succ 0.$$
 (38)

This is rewritten in the familiar form:

$$\Psi + P^T \Theta Q + Q^T \Theta P \prec 0, \quad X_{cl} = \begin{bmatrix} X & 0 & X_{13} \\ 0 & I & 0 \\ X_{13}^T & 0 & X_{33} \end{bmatrix}, X_{cl} \succ 0, \tag{39}$$

with appropriate matrices  $\Psi$ , P, Q depending on X, A, B, C and controller data gathered in

$$\Theta := \begin{bmatrix} A_K & B_K \\ C_K & D_K \end{bmatrix} .$$

We can then apply the Projection Lemma [69] to eliminate  $\Theta$ , which leads to LMI solvability conditions. There exist controllers of order  $n_K$  if and only if  $W_P^T \Psi W_P \prec 0$  and  $W_Q^T \Psi W_Q \prec 0$ , for some  $X_{cl} \succ 0$ . Introducing the inverse of  $X_{cl}$  as

$$Y_{cl} := X_{cl}^{-1} = \begin{bmatrix} Y & 0 & Y_{13} \\ 0 & I & 0 \\ Y_{13}^T & 0 & Y_{33} \end{bmatrix} ,$$

and following [69], the two projection inequalities are computed as

$$N_{C}^{T} \begin{pmatrix} A^{T} \begin{bmatrix} X & 0 \\ 0 & I \end{bmatrix} + \begin{bmatrix} X & 0 \\ 0 & I \end{bmatrix} A + \epsilon \begin{bmatrix} X & 0 \\ 0 & I \end{bmatrix} \end{pmatrix} N_{C} \prec 0$$

$$N_{B}^{T} \begin{pmatrix} A \begin{bmatrix} Y & 0 \\ 0 & I \end{bmatrix} + \begin{bmatrix} Y & 0 \\ 0 & I \end{bmatrix} A^{T} + \epsilon \begin{bmatrix} Y & 0 \\ 0 & I \end{bmatrix} \end{pmatrix} N_{B} \prec 0$$

$$(40)$$

where  $N_C$  and  $N_B$  are bases of the null space of C and  $B^T$ , respectively. Also, completion of  $X_{cl} = Y_{cl}^{-1} \succ 0$  and  $X_{cl} \in \mathbb{R}^{(n+n_K)\times(n+n_K)}$  from X and Y is equivalent to [82, 69]

$$\begin{bmatrix} X & 0 & I & 0 \\ 0 & I & 0 & I \\ I & 0 & Y & 0 \\ 0 & I & 0 & I \end{bmatrix} \succeq 0, \text{ rank } \left( I_n - \begin{bmatrix} Y & 0 \\ 0 & I_{n_{\phi}} \end{bmatrix} \begin{bmatrix} X & 0 \\ 0 & I_{n_{\phi}} \end{bmatrix} \right) \le n_K.$$
 (41)

Clearly, the maximal rank is  $\operatorname{rank}(I-YX) \leq n-n_{\phi}$  and determines the controller order. Finally, for X and Y solutions to (40) and (41), the full matrix  $X_{cl}$  can be reconstructed as well as controller state-space data  $(A_K, B_K, C_K, D_K)$  [69].

## References

- [1] H. Sussmann and P. Kokotovic, "The peaking phenomenon and the global stabilization of nonlinear systems," *IEEE Transactions on Automatic Control*, vol. 36, no. 4, pp. 424–440, 1991.
- [2] B. Francis and K. Glover, "Bounded peaking in the optimal linear regulator with cheap control," *IEEE Transactions on Automatic Control*, vol. 23, no. 4, pp. 608–617, 1978.
- [3] Z. Lin, "Co-design of linear low-and-high gain feedback and high gain observer for suppression of effects of peaking on semi-global stabilization," *Automatica*, vol. 137, p. 110124, 2022.
- [4] K. Taira, S. L. Brunton, S. T. M. Dawson, C. W. Rowley, T. Colonius, B. J. McKeon, O. T. Schmidt, S. Gordeyev, V. Theofilis, and L. S. Ukeiley, "Modal analysis of fluid flows: An overview," AIAA Journal, vol. 55, no. 12, pp. 4013–4041, 2017.
- [5] K. Taira, M. S. Hemati, S. L. Brunton, Y. Sun, K. Duraisamy, S. Bagheri, S. T. M. Dawson, and C.-A. Yeh, "Modal analysis of fluid flows: Applications and outlook," *AIAA Journal*, vol. 58, no. 3, pp. 998–1022, 2020.
- [6] P. Apkarian and D. Noll, "Optimizing the Kreiss constant," SIAM Journal on Control and Optimization, vol. 58, no. 6, pp. 3342–3362, 2020.
- [7] D. Hinrichsen and A. Pritchard, "On the transient behaviour of stable linear systems," in *Proc.* 14th International Symposium of Mathematical Theory of Networks and Systems (MTNS 2000), Perpignan, pp. 19–23, 2000.
- [8] H. Krakovska, C. Kuehn, and I. Longo, "Resilience of dynamical systems," *European Journal of Applied Math.*, vol. 35, no. 1, pp. 1–46, 2023.
- [9] M. Ghanbari and J. Jiang, "Resilience metrics in power and control systems: Comparative analysis," in *IFAC Papers Online*, vol. 58, pp. 699–704, 2024.
- [10] T. Demmer, J. Kahlen, and D. Lichte, "The use of control theory to enhance systems towards resiliance," in *Proceedings of the 33rd European Safety and Reliability Conference*, pp. 1242–1249, ESREL2023, Singapore, 2023.
- [11] J.-B. Bouvier and M. Ornik, "Resilience of linear systems to partial loss of control authority," *Automatica*, vol. 152, no. june 23, p. 110985, 2023.
- [12] J. Börner and F. Steinke, "Measuring LTI system resiliance against adversarial disturbances based on efficient eigenvalue computation," in 60th CDC21, 2021.
- [13] A. Packard and P. Seiler, "IQCs and LMIs for analysis and synthesis of uncertain systems," *IEEE Transactions on Automatic Control*, vol. 48, no. 7, pp. 1127–1143, 2003.
- [14] S. Khong and A. Lanzon, "Connections between integral quadratic constraints and dissipativity," *IEEE Trans. Autom. Contr.*, vol. 69, no. 8, pp. 5672–5677, 2024.
- [15] S. Khong, C. Chen, and A. Lanzon, "Feedback stability analysis via dissipativity with dynamic supply rates," *Automatica*, vol. 172, p. 112000, 2025.
- [16] J. Veenmann and C. Scherer, "Stability analysis with integral quadratic constraints: A dissipativity based proof," in 2013 IEEE 52nd Annual Conference on Decision and Control (CDC), (Florence, Italy), pp. 6289–6294, Dec 2013.
- [17] P. Seiler, "Stability analysis with dissipation inequalities and integral quadratic constraints," *IEEE Trans. Autom. Control.*, vol. 60, no. 6, pp. 1704–1709, 2015.
- [18] M. Xia, P. Gahinet, N. Abroug, C. Buhr, and E. Laroche, "Sector bounds in stability analysis and control design," *Int. J. Rob. Nonlin. Control*, vol. 30, pp. 7857–7882, 2020.
- [19] V. Cavalcanti and A. Simões, "IQC-synthesis under structural constraints," Int. J. Robust Nonlin. Control, vol. 30, pp. 4880–4905, 2020.

- [20] P. Apkarian and D. Noll, "IQC analysis and synthesis via nonsmooth optimization," Systems and Control Letters, vol. 55, no. 12, pp. 971–981, 2006.
- [21] A. Kalur, P. Seiler, and M. S. Hemati, "Nonlinear stability analysis of transitional flows using quadratic constraints," *Physical Review Fluids*, vol. 6, no. 4, p. 044401, 2021.
- [22] T. Mushtaq, P. J. Seiler, and M. Hemati, "Feedback stabilization of incompressible flows using quadratic constraints," in AIAA AVIATION 2022 Forum, p. 3773, 2022.
- [23] D. Astolfi, L. Marcoui, and A. Teel, "Low-power peaking-free high-gain observers for non-linear systems," 2022.
- [24] J. F. Whidborne and J. McKernan, "On the minimization of maximum transient energy growth," *IEEE Transactions on Automatic Control*, vol. 52, no. 9, pp. 1762–1767, 2007.
- [25] F. Martinelli, M. Quadrio, J. McKernan, and J. F. Whidborne, "Linear feedback control of transient energy growth and control performance limitations in subcritical plane poiseuille flow," *Phys. Fluids*, vol. 23, no. 1, p. 014103, 2011.
- [26] A. Ray, A. Pal, D. Ghosh, S. Dana, and C. Hens, "Mitigating long transient time in deterministic systems by resetting," *Chaos*, vol. 31, p. 011103, 2021.
- [27] S. Boyd, L. El Ghaoui, E. Feron, and V. Balakrishnan, Linear matrix inequalities in system and control theory. SIAM, 1994.
- [28] J. F. Whidborne, J. McKernan, and A. J. Steer, "Minimization of maximum transient energy growth by output feedback," *IFAC Proceedings Volumes*, vol. 38, no. 1, pp. 283–288, 2005.
- [29] P. Quénon and J. F. Whidborne, "Control of plane Poiseuille flow using the Kreiss constant," in *International Conference Cyber-Physical Systems and Control*, pp. 41–51, Springer, 2021.
- [30] V. Chellaboina, W. M. Haddad, D. S. Bernstein, and D. A. Wilson, "Induced convolution operator norms of linear dynamical systems," *Mathematics of Control, Signals and Systems*, vol. 13, pp. 216– 239, 2000.
- [31] F. H. Clarke, Optimization and nonsmooth analysis. SIAM, 1990.
- [32] R. J. LeVeque and L. N. Trefethen, "On the resolvent condition in the Kreiss matrix theorem," BIT Numerical Mathematics, vol. 24, no. 4, pp. 584–591, 1984.
- [33] T. Mitchell, "Computing the Kreiss constant of a matrix," SIAM Journal on Matrix Analysis and Applications, vol. 41, no. 4, pp. 1944–1975, 2020.
- [34] T. Mitchell, "Fast interpolation-based globality certificates for computing Kreiss constants and the distance to uncontrollability," SIAM Journal on Matrix Analysis and Applications, vol. 42, no. 2, pp. 578–607, 2021.
- [35] L. N. Trefethen and M. Embree, Spectra and pseudospectra, the behavior of nonnormal matrices and operators. Princeton University Press, 2005.
- [36] H. Krakovská, C. Kühn, and I. Longo, "Resilience of dynamical systems," European Journal of Applied Mathematics, 2024.
- [37] S. Lee and P. S. Marcus, "Linear stability analysis of wake vortices by a spectral method using mapped legendre functions," *Journal of Fluid Mechanics*, vol. 967, p. A2, 2023.
- [38] P. S. Shcherbakov and F. Dabbene, "A probabilistic point of view on peak effects in linear difference equations," *European Journal of Control*, vol. 63, pp. 107–115, 2022.
- [39] N. A. García Hilares, Mathematical Modeling and Dynamic Recovery of Power Systems. PhD thesis, Virginia Polytechnic Institute and State University, Blacksburg, VA, USA, 2023.
- [40] S. Lee, "Linear stability of a wake vortex and its transient growth," Master's thesis, University of California, Berkeley, 2024.
- [41] N. Dudarenko, N. Vunder, V. Melnikov, and A. Zhilenkov, "Minimization of peak effect in the free motion of linear systems with restricted control," *Informatics and Automation*, vol. 22, no. 3, 2023.
- [42] P. Apkarian and D. Noll, "Optimization-based control design techniques and tools," in *Encyclopedia of Systems and Control* (J. Baillieul and T. Samad, eds.), pp. 1626–1637, Springer, Cham, 2021.
- [43] P. Apkarian, M. N. Dao, and D. Noll, "Parametric robust structured control design," *Automatic Control, IEEE Transactions on*, vol. 60, no. 7, pp. 1857–1869, 2015.
- [44] P. Apkarian and D. Noll, "Worst-case stability and performance with mixed parametric and dynamic uncertainties," *International Journal of Robust and Nonlinear Control*, vol. 27, no. 8, pp. 1284–1301, 2017.
- [45] P. Apkarian and D. Noll, "Nonsmooth  $H_{\infty}$  synthesis," *IEEE Transactions on Automatic Control*, vol. 51, no. 1, pp. 71–86, 2006.
- [46] P. Apkarian and D. Noll, "Nonsmooth optimization for multidisk  $H_{\infty}$  synthesis," European Journal of Control, vol. 12, no. 3, pp. 229–244, 2006.

- [47] H. J. Brascamp and E. H. Lieb, "Best constants in Young's inequality, its converse, and its generalization to more than three functions," *Advances in Mathematics*, vol. 20, no. 2, pp. 151–173, 1976.
- [48] S. Boyd and C. Barratt, Linear Controller Design: Limits of Performance. Prentice-Hall, 1991.
- [49] M. Spijker, "On a conjecture by Leveque and Trefethen related to the Kreiss matrix theorem," BIT Numerical Mathematics, vol. 31, pp. 551–555, 1991.
- [50] H.-O. Kreiss, "Über die Stabilitätsdefinition für Differenzengleichungen die partielle Differentialgleichungen approximieren," *BIT Numerical Mathematics*, vol. 2, pp. 153–181, 1962.
- [51] K.-J. Engel, R. Nagel, and S. Brendle, One-parameter semigroups for linear evolution equations, vol. 194. Springer, 2000.
- [52] D. Swaroop and D. Neimann, "On the impulse response of LTI systems," in *Proceedings of the 2001 American Control Conference*. (Cat. No. 01CH37148), vol. 1, pp. 523–528, IEEE, 2001.
- [53] L. N. Trefethen, A. E. Trefethen, S. C. Reddy, and T. A. Driscoll, "Hydrodynamic stability without eigenvalues," *Science*, vol. 261, no. 5121, pp. 578–584, 1993.
- [54] D. Hinrichsen and A. Pritchard, "On the transient behaviour of stable linear systems," Proc. Int. Symp. Math. Theory Networks & Syst. Perpignan, France. CDROM paper B218., vol. 2, p. 2, 2000.
- [55] P. J. Schmid and L. Brandt, "Analysis of fluid systems: Stability, receptivity, sensitivity. Lecture Notes from the flow-nordita summer school on advanced instability methods for complex flows, Stockholm, Sweden, 2013," Applied Mechanics Reviews, vol. 66, no. 2, p. 024803, 2014.
- [56] P. Apkarian and D. Noll, "Controller design via nonsmooth multi-directional search," SIAM J. on Control and Optimization, vol. 44, no. 6, pp. 1923–1949, 2006.
- [57] P. Apkarian and D. Noll, "Nonsmooth optimization for multiband frequency domain control design," *Automatica*, vol. 43, no. 4, pp. 724 731, 2007.
- [58] "Robust control toolbox 6.11," 2021. The MathWorks, Natick, MA, USA.
- [59] S. Boyd and J. Doyle, "Comparison of peak and RMS gains for discrete-time systems," Systems & Control Letters, vol. 9, no. 1, pp. 1–6, 1987.
- [60] J. Doyle and C. C. Chu, "Robust control of multivariable and large scale systems," Tech. Rep. AD-A175 058, Honeywell Systems and Research center, 1986.
- [61] P. Apkarian and D. Noll, "Mixed  $L_1/H_{\infty}$ -synthesis for  $L_{\infty}$ -stability," International Journal of Robust and Nonlinear Control, vol. 32, no. 4, pp. 2119–2142, 2022.
- [62] M. Dao and D. Noll, "Minimizing the memory of a system," *Mathematics of Control, Signals and Systems*, vol. 27, no. 1, pp. 77–110, 2015.
- [63] S. L. Brunton and B. R. Noack, "Closed-loop turbulence control: Progress and challenges," Applied Mechanics Reviews, vol. 67, no. 5, 2015.
- [64] C. Leclercq, F. Demourant, C. Poussot-Vassal, and D. Sipp, "Linear iterative method for closed-loop control of quasiperiodic flows," *Journal of Fluid Mechanics*, vol. 868, pp. 26–65, 2019.
- [65] S. J. Illingworth, A. S. Morgans, and C. W. Rowley, "Feedback control of cavity flow oscillations using simple linear models," *Journal of Fluid Mechanics*, vol. 709, p. 223–248, 2012.
- [66] K. Zhou, J. C. Doyle, and K. Glover, Robust and Optimal Control. Prentice Hall, 1996.
- [67] E. N. Lorenz, "Deterministic nonperiodic flow," Journal of Atmospheric Sciences, vol. 20, no. 2, pp. 130–141, 1963.
- [68] C. Liu and D. F. Gayme, "Input-output inspired method for permissible perturbation amplitude of transitional wall-bounded shear flows," *Physical Review E*, vol. 102, no. 6, p. 063108, 2020.
- [69] P. Gahinet and P. Apkarian, "A linear matrix inequality approach to  $H_{\infty}$  control," International Journal of Robust and Nonlinear Control, vol. 4, no. 4, pp. 421–448, 1994.
- [70] J. F. Sturm, "Using sedumi 1.02, a matlab toolbox for optimization over symmetric cones," Optimization methods and software, vol. 11, no. 1-4, pp. 625–653, 1999.
- [71] J. S. Li, Y. L. Zhou, S. B. Shi, and H. Q. Liu, "Multivariable control of a supercritical boiler with load regulation using loop shaping and LMI-based robust control," *IEEE Access*, vol. 11, pp. 17822–17834, 2023.
- [72] D. H. Lim, S. H. Lee, and J. Y. Kim, "Active vibration control of a high-speed railway pantograph using  $H_{\infty}$  and systume methods," *Journal of Mechanical Science and Technology*, vol. 36, no. 10, pp. 4773–4781, 2022.
- [73] D. L. Vilarino, F. B. G. A. de Sousa, and E. H. C. Junior, "Multivariable control of a wind turbine to minimize loads using the  $H_{\infty}/\mu$ -synthesis and the systume functions," *Journal of Control, Automation and Electrical Systems*, vol. 33, no. 5, pp. 1117–1129, 2022.

- [74] G. Le Guehennec, J. Verron, and N. Petit, "Robust  $H_{\infty}$  control design for a satellite attitude control system," *IFAC-PapersOnLine*, vol. 53, no. 2, pp. 11175–11181, 2020.
- [75] R. Maheshwari, A. Kumar, and S. Sharma, "Robust flight control design for a launch vehicle using structured  $H_{\infty}$  synthesis," Journal of Aerospace Engineering, vol. 35, no. 2, p. 04021110, 2022.
- [76] F. B. G. A. de Sousa, M. R. V. de Castro, and M. W. S. Maudsley, "Robust control law for a european launcher in the ascent phase," *Journal of Aerospace Engineering*, vol. 34, no. 4, p. 04021029, 2021.
- [77] M. I. Asghar, S. S. Kim, and I. H. Lim, "Multivariable robust control of a large wind turbine using the  $H_{\infty}$  synthesis technique," *Journal of Control, Automation and Systems*, vol. 21, no. 10, pp. 3129–3138, 2023.
- [78] J. Zabczyk, Mathematical Control Theory: an introduction. Birkhäuser, Boston, 2008.
- [79] J. A. Yorke, "A theorem on Liapunov functions using  $\ddot{V}$ ," Mathematical Systems Theory, vol. 4, no. 1, pp. 40–45, 1970.
- [80] A. A. Ahmadi and P. A. Parrilo, "On higher order derivatives of Lyapunov functions," in *Proceedings* of the 2011 American Control Conference, pp. 1313–1314, IEEE, 2011.
- [81] A. Papachristodoulou, J. Anderson, G. Valmorbida, S. Prajna, P. Seiler, P. A. Parrilo, M. M. Peet, and D. Jagt, SOSTOOLS: Sum of squares optimization toolbox for MATLAB. http://arxiv.org/abs/1310.4716, 2021. Available from https://github.com/oxfordcontrol/SOSTOOLS.
- [82] A. Packard, K. Zhou, P. Pandey, and G. Becker, "A collection of robust control problems leading to LMIs," in [1991] Proceedings of the 30th IEEE Conference on Decision and Control, pp. 1245–1250, IEEE, 1991.